

國 立 清 華 大 學
碩 士 論 文

雙黑洞在星系重力場下的速度比之研究

The Study on the Velocity Ratio of Binary Black
Holes with Galactic Potential



系所：計算與建模科學研究所

學號：110026501

研究生：林凌豪 (Lin-Hao Lin)

指導教授：葉麗琴 (Li-Chin Yeh)

中華民國 一百一十二年 六月

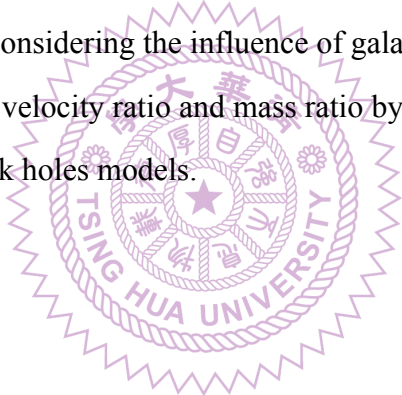
摘要

在本論文中，主要探討雙黑洞動態系統在星系重力場的影響下，速度比與質量比之間的關係。在天文學的研究裡，普遍認為活躍星系核中心是超大質量黑洞。Wang et al. [11] 在雙活躍星系核的研究中，發現雙活躍星系核速度比與質量比之間有著顯著的相關性。因此，在考慮星系重力場的影響下，我們提供不同初始條件的雙黑洞模型，對速度比與質量比的關係進行研究。



Abstract

In this thesis, we primarily study the relationship between velocity ratio and mass ratio in the binary black holes with galactic potential. In the field of astronomy, it is widely accepted that the center of active galactic nuclei hosts supermassive black hole. In the study of dual active galactic nuclei (AGNs), Wang et al. [11] discovered a significant correlation between the velocity ratio and mass ratio of dual AGNs. Therefore, considering the influence of galactic potential, we explore the relationship between velocity ratio and mass ratio by choosing different initial conditions in binary black holes models.



Acknowledgements

研究所在學期間，我要向所有幫助過我的人致以最衷心的感謝，他們的支持和鼓勵對於我兩年的研究生活具有重要意義。

首先，我要感謝葉麗琴教授，在寫作論文時，她給予我寶貴的指導和建議，尤其我在念研究所之前，對於天文學的專業知識尚淺，教授依然耐心且無私地與我討論，給予珍貴的意見，使我在研究中能夠不斷改進和成長。

我還要感謝論文口試委員江瑛貴教授與陳賢修教授，不僅撥冗參加我的論文口試，口試時還提供了許多可貴的建議，使我獲益良多。

最後，我要感謝我的家人和朋友，他們在我整個研究生涯中給予了無限的支持和鼓勵。在此，我要特別感謝我的祖母，沒有她，這一切根本不可能發生。

林凌豪 謹致於 國立清華大學
計算與建模科學研究所
中華民國一一二年七月一日

Contents

摘要	i
Abstract	ii
Acknowledgements	
1 Introduction	1
2 Analytical Formulas	3
2.1 Circular Orbit	3
2.2 Elliptical Orbit	7
3 The Orbit Behaviors of Supermassive Binary Black Hole in Galaxical Potential	14
3.1 Equations of Motion	16
3.2 $\mathbf{c} = \mathbf{0}$ Case with a circular orbit	19
3.3 $\mathbf{c} \neq \mathbf{0}$ Case with elliptical orbits	22
3.3.1 Equal mass case	22
3.3.2 Unequal masses cases	24
3.3.3 Different total mass of galaxy	31
4 Conclusion	33
A Kepler's Laws of Planetary Motion	34
A.1 Kepler's 2nd Law	34
A.2 Kepler's 1st Law	36
A.3 Kepler's 3rd Law	39
B Three Dimensional Transformation	41
References	43

List of Figures

2.1	Binary system with circular orbits.	3
2.2	Inclination of an orbit.	6
2.3	Orbital motion and reference plane in three-dimensional space.	7
2.4	The position vector of the two particles P_1, P_2 with mass m_1, m_2 respectively, with respect to the origin, O , and with respect to the centre of mass, O'	10
2.5	Centre of mass coordinate system of P_1 in three-dimensional space.	12
3.1	The total energy from $t = 0$ to $t = 100$	20
3.2	Case of $c = 0$. (a) The orbit on $\hat{X}\hat{Y}$ -plane from $t = 0$ to $t = 100$. (b) The orbit on $\hat{X}\hat{Z}$ -plane from $t = 0$ to $t = 100$. (c) The length of r_{12} from $t = 0$ to $t = 100$. (d) The orbital radial velocity ratio from $t = 0$ to $t = 100$	21
3.3	Orbital plots of Model A1 and Model A2. (a) The Model A1 orbit on $\hat{X}\hat{Y}$ -plane from $t = 0$ to $t = 100$. (b) The Model A1 orbit on $\hat{X}\hat{Z}$ -plane from $t = 0$ to $t = 100$. (c) The Model A2 orbit on $\hat{X}\hat{Y}$ -plane from $t = 0$ to $t = 100$. (d) The Model A2 orbit on $\hat{X}\hat{Z}$ -plane from $t = 0$ to $t = 100$	23
3.4	The length of r_{12} from $t = 0$ to $t = 100$	23
3.5	Orbital plots of Model B1 and Model B2. (a) The Model B1 orbit on $\hat{X}\hat{Y}$ -plane from $t = 0$ to $t = 100$. (b) The Model B1 orbit on $\hat{X}\hat{Z}$ -plane from $t = 0$ to $t = 100$. (c) The Model B2 orbit on $\hat{X}\hat{Y}$ -plane from $t = 0$ to $t = 100$. (d) The Model B2 orbit on $\hat{X}\hat{Z}$ -plane from $t = 0$ to $t = 100$	25
3.6	The length of r_{12} from $t = 0$ to $t = 100$	26
3.7	The orbital radial velocity ratio from $t = 0$ to $t = 100$. (a) The Model B1. (b) The Model B2.	26
3.8	Orbital plots of Model C1 and Model C2. (a) The Model C1 orbit on $\hat{X}\hat{Y}$ -plane from $t = 0$ to $t = 100$. (b) The Model C1 orbit on $\hat{X}\hat{Z}$ -plane from $t = 0$ to $t = 100$. (c) The Model C2 orbit on $\hat{X}\hat{Y}$ -plane from $t = 0$ to $t = 100$. (d) The Model C2 orbit on $\hat{X}\hat{Z}$ -plane from $t = 0$ to $t = 100$	27
3.9	The length of r_{12} from $t = 0$ to $t = 100$	27
3.10	The orbital radial velocity ratio from $t = 0$ to $t = 100$. (a) The Model C1. (b) The Model C2.	28
3.11	Orbital plots of Model D1 and Model D2. (a) The Model D1 orbit on $\hat{X}\hat{Y}$ -plane from $t = 0$ to $t = 100$. (b) The Model D1 orbit on $\hat{X}\hat{Z}$ -plane from $t = 0$ to $t = 100$. (c) The Model D2 orbit on $\hat{X}\hat{Y}$ -plane from $t = 0$ to $t = 100$. (d) The Model D2 orbit on $\hat{X}\hat{Z}$ -plane from $t = 0$ to $t = 100$	29
3.12	The length of r_{12} from $t = 0$ to $t = 100$	29
3.13	The orbital radial velocity ratio from $t = 0$ to $t = 100$. (a) The Model D1. (b) The Model D2.	30
3.14	The galaxical potentials V from $r = 0.002$ to $r = 2$	31
3.15	The orbital radial velocity ratio with $E_0 = -E_{total}^c/2$ from $t = 0$ to $t = 15$	32

3.16 The orbital radial velocity ratio with $E_0 = -E_{total}^c/18$ from $t = 0$ to $t = 15$.	32
A.1 A vector diagram for the forces acting on two particles with position vectors ([10], p.23).	34
B.1 The relation between the orbital plane system $(\hat{x}, \hat{y}, \hat{z})$ and the reference plane system $(\hat{X}, \hat{Y}, \hat{Z})$ ([10], p.50). (a) The originally coincident axes. (b) The first rotation. (c) The second rotation. (d) The final rotation.	41



List of Tables

3.1	Model with $m_1 = m_2 = 0.5$.	22
3.2	Models with $m_1 = \alpha, m_2 = 1 - \alpha$.	25
A.1	Types of orbit ([10], p.26).	38



Chapter 1

Introduction

The existence of a supermassive black hole at the galactic nucleus is widely acknowledged. In the event of a merger between two galaxies harboring supermassive black holes, it is highly probable that a pair of supermassive binary black holes (SMBBH) will form in close proximity to the central region of the resultant galactic merger.

In the investigation of dual active galactic nuclei, Wang et al. [11] identified a significant correlation between the velocity ratio and mass ratio of these dual active galactic nuclei explained by Keplerian diagram. This prompts us to examine the outcomes of the binary black holes model within the framework of galactic potential.

In order to investigate the binary black hole model, In Chapter 2 we introduce a framework where the model is treated as a two-body problem, allowing us to explore the relation between the mass ratio and velocity ratio of the two particles. In Section 2.1 we focus on the specific case of a circular orbit in xy -plane, providing insights into the dynamics of the two-body problem. Following that, in Section 2.2 we extend the analysis to the scenario of elliptical orbits in three-dimensional space, with particular emphasis on examining the relationship between mass ratio and velocity ratio. The radial velocity along the z-axis serves as an observable indicator in this discussion.

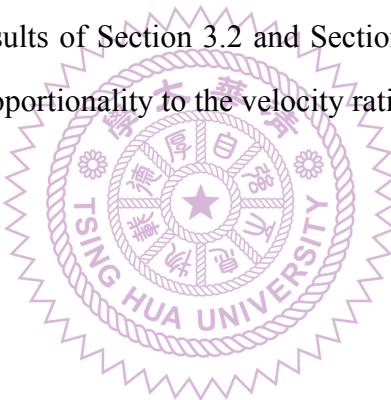
In Chapter 3, we initiate a discourse concerning the incorporation of galactic potential into the two-body problem and the development of our binary black holes model. By considering several initial conditions, we explore a range of model outcomes. Jiang and Yeh [3] formulated

a theoretical framework encompassing a SMBH embedded in the galactic center. The selected galactic density profile adheres to the Nuker law (Lauer et al. [6] and Jiang and Yeh [3]),

$$\rho(r) = \rho_c r^{-\gamma} (1 + r^\alpha)^{(\gamma - \beta)/\alpha}.$$

In this study, we set the parameters $\alpha = 2$, $\beta = 4$, and $\gamma = 0$, which is Kandrup potential model (Kandrup et al. [4]). In Section 3.1, we construct binary black holes model with Kandrup potential and calculate the formula of total energy. Firstly, in Section 3.2, we consider the case of circular orbits and show the result of relationship between mass ratio and velocity ratio by Runge-Kutta 4th order method (RK4). Subsequently, in Section 3.3, we explore the case of elliptical orbits by considering different initial total energies and the masses of particles. Then, the result of relationship between mass ratio and velocity ratio is presented.

Based on the numerical results of Section 3.2 and Section 3.3, the mass ratio of the two particles exhibits an inverse proportionality to the velocity ratio.



Chapter 2

Analytical Formulas

In this chapter, we introduce some concepts of two-body problem and derive the equations to present some analytical formulas for the relations between the orbital velocity ratio and the mass ratio of supermassive binary black hole without galactical potential.

2.1 Circular Orbit

In this section, the equation of motion for two-body problem in circular orbits will be presented (Murray and Dermott [10]) Suppose that there are two particles P_1, P_2 , of masses m_1, m_2 , orbiting their common center of mass (CM) at distances R_1, R_2 with velocities \vec{v}_1 and \vec{v}_2 respectively (see Figure 2.1).

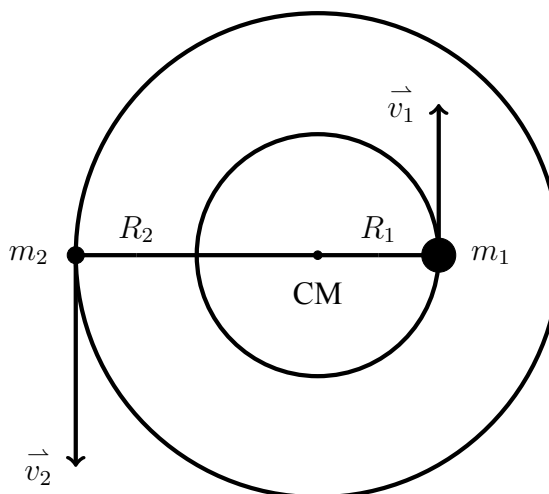


Figure 2.1: Binary system with circular orbits.

From definition of center of mass, we could get

$$m_1 R_1 = m_2 R_2. \quad (2.1)$$

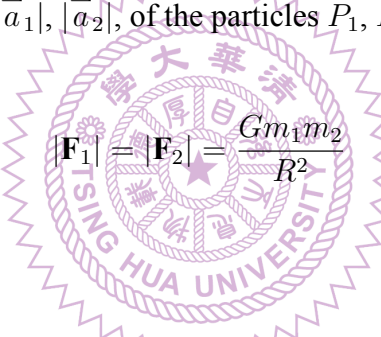
Let R be the distance between particle P_1 and P_2 . Then

$$R = R_1 + R_2. \quad (2.2)$$

From Eq.(2.1) and Eq.(2.2), we know that

$$R_1 = \frac{m_2}{m_1 + m_2} R, \quad \text{and} \quad R_2 = \frac{m_1}{m_1 + m_2} R. \quad (2.3)$$

Now, we apply Newton's law of gravity. Then the values of gravitational force, $|\mathbf{F}_1|$, $|\mathbf{F}_2|$, and the values of acceleration, $|\vec{a}_1|$, $|\vec{a}_2|$, of the particles P_1 , P_2 are



$$|\mathbf{F}_1| = |\mathbf{F}_2| = \frac{G m_1 m_2}{R^2} \quad (2.4)$$

and

$$|\vec{a}_1| = \frac{G m_2}{R^2} \quad \text{and} \quad |\vec{a}_2| = \frac{G m_1}{R^2}, \quad (2.5)$$

where G is the universal gravitational constant. From Eq.(2.3), we have

$$m_1 = \frac{R_2}{R} (m_1 + m_2) \quad \text{and} \quad m_2 = \frac{R_1}{R} (m_1 + m_2). \quad (2.6)$$

Using the result of Eq.(2.4) and Eq.(2.6), the value of gravitational force of P_1 and P_2 are

$$|\mathbf{F}_1| = \frac{G m_1 m_2}{R^2} = m_1 \cdot \frac{G((m_1 + m_2) R_1 / R)}{R^2} = m_1 \cdot R_1 \frac{G(m_1 + m_2)}{R^3}, \quad (2.7)$$

and

$$|\mathbf{F}_2| = \frac{G m_1 m_2}{R^2} = m_2 \cdot \frac{G((m_1 + m_2) R_2 / R)}{R^2} = m_2 \cdot R_2 \frac{G(m_1 + m_2)}{R^3}. \quad (2.8)$$

Since $|\mathbf{F}_1| = |\mathbf{F}_2|$ and from Eq.(2.7) and Eq.(2.8), then

$$m_1 \cdot R_1 = m_2 \cdot R_2. \quad (2.9)$$

Moreover from Eq.(2.9),

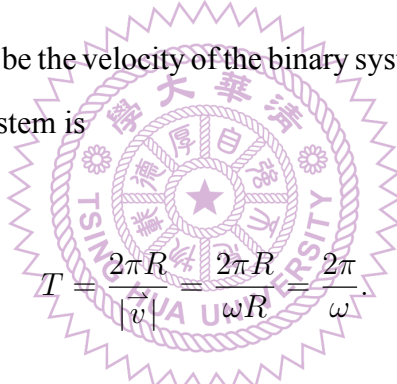
$$\frac{m_1}{m_2} = \frac{R_2}{R_1}. \quad (2.10)$$

From Eq.(2.7) and Eq.(2.8), the angular velocity of the binary system ω , is

$$\omega = \sqrt{\frac{G(m_1 + m_2)}{R^3}}. \quad (2.11)$$

Then, from Eq.(2.11), and let \vec{v} be the velocity of the binary system using the relation $|\vec{v}| = \omega R$.

Then the period T of binary system is



$$T = \frac{2\pi R}{|\vec{v}|} = \frac{2\pi R}{\omega R} = \frac{2\pi}{\omega}. \quad (2.12)$$

Furthermore, if we consider the circular orbits of P_1 and P_2 , from Eq.(2.12), then the circumferences of P_1 and P_2 are

$$2\pi R_1 = |\vec{v}_1|T, \quad \text{and} \quad 2\pi R_2 = |\vec{v}_2|T. \quad (2.13)$$

From Eq.(2.13), we could obtain

$$|\vec{v}_1| = \frac{2\pi R_1}{T}, \quad \text{and} \quad |\vec{v}_2| = \frac{2\pi R_2}{T}. \quad (2.14)$$

Heretofore, we have been considering the situation in which the observer is in the plane of the system orbit. Consider the observer is not in the plane of the system orbit.

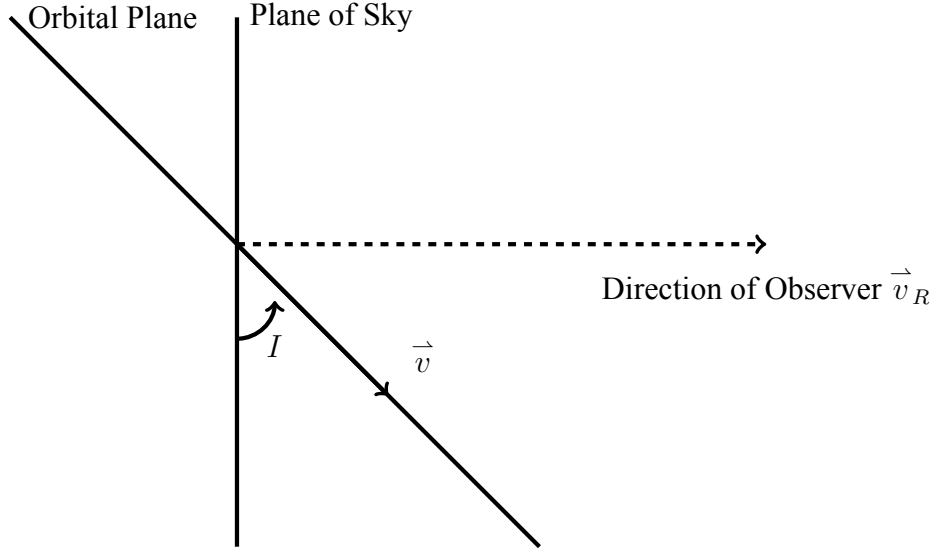


Figure 2.2: Inclination of an orbit.

If I is the angle between the plane of the orbit and the plane of the sky, then the projection of velocity \vec{v} in the plane of the orbit into the line of direction of observe is \vec{v}_R (see Figure 2.2), i.e.

$$\vec{v}_R = \vec{v} \cos(90^\circ - I) = \vec{v} \sin(I). \quad (2.15)$$

Hence, from Eq.(2.15), the line of direction of observes of \vec{v}_1 and \vec{v}_2 are \vec{v}_{R_1} and \vec{v}_{R_2} , is below :

$$\vec{v}_{R_1} = \vec{v}_1 \sin(I), \quad \text{and} \quad \vec{v}_{R_2} = \vec{v}_2 \sin(I). \quad (2.16)$$

Therefore, from Eq.(2.10), Eq.(2.14), and Eq.(2.16), we obtain that

$$\frac{|\vec{v}_{R_1}|}{|\vec{v}_{R_2}|} = \frac{|\vec{v}_1 \sin(I)|}{|\vec{v}_2 \sin(I)|} = \frac{2\pi R_1/T}{2\pi R_2/T} = \frac{R_1}{R_2} = \frac{m_2}{m_1},$$

which could know that the relation between the observe of orbital velocity ratio and the mass ratio of binary system, is

$$\frac{|\vec{v}_{R_1}|}{|\vec{v}_{R_2}|} = \frac{m_2}{m_1}. \quad (2.17)$$

2.2 Elliptical Orbit

In this section, we show the three-dimensional representation of an elliptical orbit in space. We consider a three-dimensional Cartesian coordinate system where the direction of the reference line in the reference plane forms the \hat{X} -axis. The \hat{Y} -axis is in the reference plane at right-angles to the \hat{X} -axis, while the \hat{Z} -axis is perpendicular to both the \hat{X} - and \hat{Y} -axes forming a right-handed triad (see Figure 2.3).

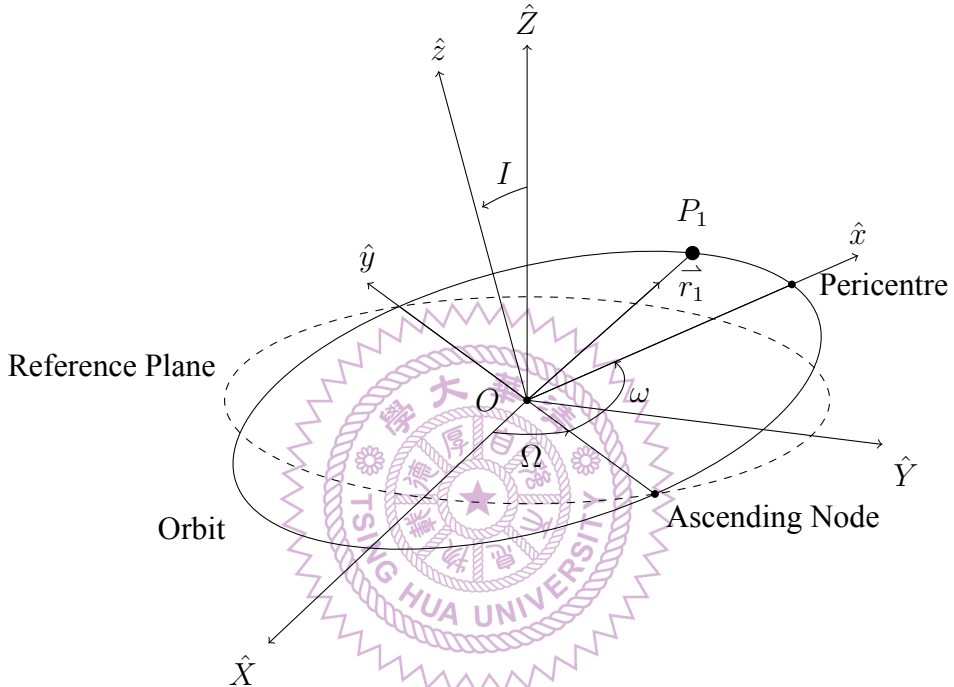


Figure 2.3: Orbital motion and reference plane in three-dimensional space.

Firstly, we define some elements of celestial mechanics in Figure 2.3. Generally, the orbital plane will be inclined to the reference plane at an angle $I \in [0, \pi]$ called the inclination of the orbit. The point in reference plane and orbital plane whose orbit crosses the reference plane moving from below to above the plane is called the ascending node. The angle between the reference line and the radius vector of orbit, \vec{r}_1 , to the ascending node is called the longitude of ascending node, denoted Ω . The angle between this same radius vector and the pericentre of the orbit is called the argument of pericentre, denoted ω . Then defining the angle ϖ is called the longitude of pericentre, that is,

$$\varpi = \Omega + \omega,$$

as $I \rightarrow 0$. From Eq.(A.19) and Table A.1 of Appendix A.2, we could suppose that the elliptical motion in polar coordinate system, i.e.

$$|\vec{r}_1| = \frac{a(1 - e^2)}{1 + e \cos(\theta - \varpi)}, \quad (2.18)$$

where e is the eccentricity and θ is called the true longitude, which is the angle between the reference line and the radius vector. Moreover, we let f be the true anomaly, i.e.

$$f = \theta - \varpi. \quad (2.19)$$

Hence, we differentiate Eq.(2.19) with respect to the time t , we have

$$\dot{f} = \dot{\theta} = \frac{d\theta}{dt}. \quad (2.20)$$

From Eq.(2.19), we also could rewrite Eq.(2.18) to be

$$|\vec{r}_1| = \frac{a(1 - e^2)}{1 + e \cos(f)}. \quad (2.21)$$

Suppose that there are two particles P_1, P_2 with mass m_1, m_2 , and with position vectors \vec{r}_1, \vec{r}_2 referred to some origin O fixed in inertial space. Furthermore, let orbital radius vector $\vec{r} = \vec{r}_2 - \vec{r}_1$ denotes the relative position of the particle P_2 with respect to P_1 (see Figure A.1), and let $\mu = G(m_1 + m_2)$ where G is the universal gravitational constant. From Eq.(A.22) in Appendix A.3, we obtain that

$$T^2 = \frac{4\pi^2}{\mu} a^3, \quad (2.22)$$

where T is one orbital period and a is the semi-major axis. We define average angular velocity, n ,

$$n = \frac{2\pi}{T}.$$

Then Eq.(2.22) could rewrite to

$$\mu = \frac{4\pi^2}{T^2} a^3 = n^2 a^3. \quad (2.23)$$

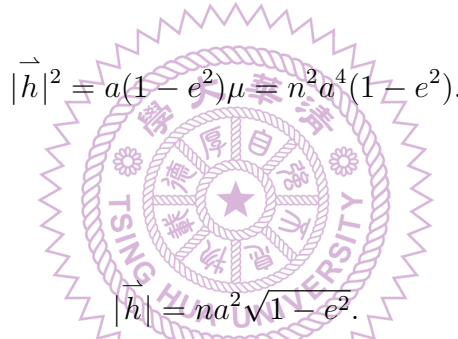
From Eq.(A.10) in Appendix A.1, by using the result of Eq.(2.20), we can obtain that

$$|\vec{h}| = |\vec{r}|^2 \dot{\theta} = |\vec{r}|^2 \dot{f}. \quad (2.24)$$

Moreover, from Eq.(A.19) in Appendix A.2, we know that $p = |\vec{h}|^2/\mu$ and from Table A.1 if the orbit is elliptical, then we have $p = a(1 - e^2)$. Then we get

$$|\vec{h}|^2 = p\mu = a(1 - e^2)\mu. \quad (2.25)$$

Using result of Eq.(2.23), we rewrite Eq.(2.25) to become



$$|\vec{h}|^2 = a(1 - e^2)\mu = n^2 a^4 (1 - e^2).$$

$$|\vec{h}| = na^2 \sqrt{1 - e^2}.$$
(2.26)

Thus, we have

$$|\vec{r}| \dot{f} = \frac{|\vec{h}|}{|\vec{r}|} = na^2 \sqrt{1 - e^2} \cdot \frac{1}{|\vec{r}|} = na^2 \sqrt{1 - e^2} \cdot \frac{1 + e \cos(f)}{a(1 - e^2)} = \frac{na(1 + e \cos(f))}{\sqrt{1 - e^2}}. \quad (2.27)$$

We differentiate Eq.(2.21) with respect to the time t , then

$$\dot{|\vec{r}|} = \frac{-a(1 - e^2)(-e \sin(f))}{(1 + e \cos(f))^2} \dot{f} = |\vec{r}| \dot{f} \frac{e \sin(f)}{1 + e \cos(f)}. \quad (2.28)$$

Since the result of Eq.(2.27), we have

$$\dot{|\vec{r}|} = |\vec{r}| \dot{f} \frac{e \sin(f)}{1 + e \cos(f)} = \frac{na(1 + e \cos(f))}{\sqrt{1 - e^2}} \cdot \frac{e \sin(f)}{1 + e \cos(f)} = \frac{nae \sin(f)}{\sqrt{1 - e^2}}. \quad (2.29)$$

Now, we consider the particle P_2 position at orbital plane in Cartesian system, $(\vec{x}, \vec{y}, \vec{z}) = (|\vec{r}| \cos(f), |\vec{r}| \sin(f), 0)$, then from Appendix B, the position of P_2 at reference plane is

$$\begin{aligned} \begin{pmatrix} \vec{X} \\ \vec{Y} \\ \vec{Z} \end{pmatrix} &= \mathbf{P}_3 \mathbf{P}_2 \mathbf{P}_1 \begin{pmatrix} \vec{x} \\ \vec{y} \\ \vec{z} \end{pmatrix} \\ &= \mathbf{P}_3 \mathbf{P}_2 \mathbf{P}_1 \begin{pmatrix} \vec{r} \cos(f) \\ \vec{r} \sin(f) \\ 0 \end{pmatrix} \\ &= \vec{r} \begin{pmatrix} \cos(\Omega) \cos(\omega + f) - \sin(\Omega) \sin(\omega + f) \cos(I) \\ \sin(\Omega) \cos(\omega + f) + \cos(\Omega) \sin(\omega + f) \cos(I) \\ \sin(\omega + f) \sin(I) \end{pmatrix}. \end{aligned} \quad (2.30)$$

Next, we use a centre of mass coordinate system with origin at the point O' (see Figure 2.4).

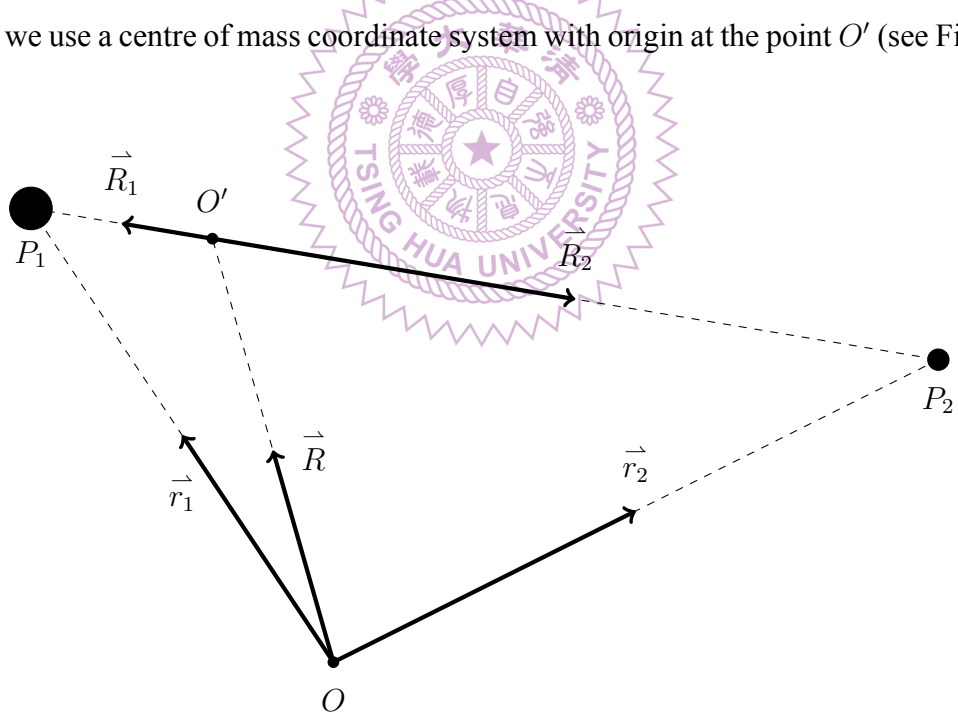


Figure 2.4: The position vector of the two particles P_1, P_2 with mass m_1, m_2 respectively, with respect to the origin, O , and with respect to the centre of mass, O' .

Let \vec{R} denote the position vector of the centre of mass O' , referred to the fixed origin O . Then, from Figure 2.4, the relation of the vector \vec{R} could be written as

$$m_1 \vec{r}_1 + m_2 \vec{r}_2 - (m_1 + m_2) \vec{R} = 0, \quad (2.31)$$

and we define

$$\vec{R}_1 = \vec{r}_1 - \vec{R}, \quad \text{and} \quad \vec{R}_2 = \vec{r}_2 - \vec{R}. \quad (2.32)$$

From Eq.(2.31) and Eq.(2.32), we get

$$m_1 \vec{R}_1 + m_2 \vec{R}_2 = 0. \quad (2.33)$$

Assume $r = |\vec{R}_1| + |\vec{R}_2|$ and from Eq.(2.31)-(2.33), we obtain

$$\begin{aligned} |\vec{R}_1| &= \frac{m_2}{m_1} |\vec{R}_2| = \frac{m_2}{m_1} |\vec{r}_2 - \vec{R}| = \frac{m_2}{m_1} |\vec{r}_2 - \frac{m_1 \vec{r}_1 + m_2 \vec{r}_2}{m_1 + m_2}| \\ &= \frac{m_2}{m_1} \cdot \frac{m_1}{m_1 + m_2} |\vec{r}_2 - \vec{r}_1| = \frac{m_2}{m_1} \cdot \frac{m_1}{m_1 + m_2} r = \frac{m_2}{m_1 + m_2} r. \end{aligned} \quad (2.34)$$

Similarly,

$$|\vec{R}_2| = \frac{m_1}{m_2} |\vec{R}_1| = \frac{m_1}{m_2} \cdot \frac{m_2}{m_1 + m_2} r = \frac{m_1}{m_1 + m_2} r. \quad (2.35)$$

Thus, from Eq.(2.34) and Eq.(2.35), we could have

$$\vec{R}_1 = -\frac{m_2}{m_1 + m_2} \vec{r}, \quad \text{and} \quad \vec{R}_2 = +\frac{m_1}{m_1 + m_2} \vec{r}. \quad (2.36)$$

Finally, we consider the observer take the reference plane (\hat{X}, \hat{Y}) to be the plane of the sky perpendicular to the line of sight, the \hat{Z} -axis oriented towards the observer (see Figure 2.5).

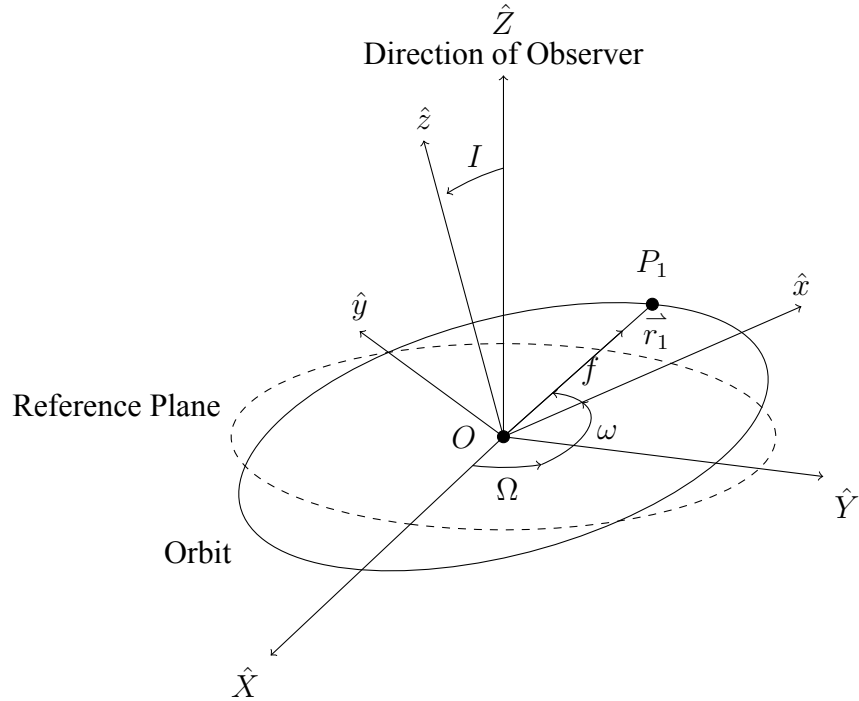


Figure 2.5: Centre of mass coordinate system of P_1 in three-dimensional space.

The velocity of particle P_1 projection on the \hat{Z} -axis, $\vec{v}_{1,\hat{z}}$, is presented (Murray and Correia [9]) as below,

$$\vec{v}_{1,\hat{z}} = \frac{d}{dt}(\vec{r}_1 \cdot \hat{Z}) = \dot{\vec{r}}_1 \cdot \hat{Z}. \quad (2.37)$$

From Eq.(2.32), we rewrite Eq.(2.37) to be

$$\vec{v}_{1,\hat{z}} = (\dot{\vec{R}} + \dot{\vec{R}}_1) \cdot \hat{Z}. \quad (2.38)$$

Let $V_{\hat{Z}} = \dot{\vec{R}} \cdot \hat{Z}$. Then, from Eq.(2.38),

$$\vec{v}_{1,\hat{z}} = V_{\hat{Z}} + (\dot{\vec{R}}_1 \cdot \hat{Z}). \quad (2.39)$$

From Eq.(2.30) and Eq.(2.36),

$$\dot{\vec{R}}_1 \cdot \hat{Z} = -\frac{d}{dt}\left(\frac{m_2}{m_1 + m_2} \vec{r} \cdot \hat{Z}\right) = -\frac{d}{dt}\left(\frac{m_2}{m_1 + m_2} r \sin(\omega + f) \sin(I)\right). \quad (2.40)$$

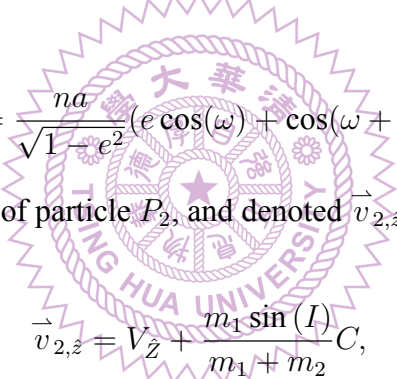
Then, using the result of Eq.(2.40), Eq.(2.39) could be

$$\begin{aligned}\vec{v}_{1,\hat{z}} &= V_{\hat{Z}} - \frac{d}{dt} \left(\frac{m_2}{m_1 + m_2} r \sin(\omega + f) \sin(I) \right) \\ &= V_{\hat{Z}} - \frac{m_2 \sin(I)}{m_1 + m_2} (\dot{r} \sin(\omega + f) + r \dot{f} \cos(\omega + f)).\end{aligned}\quad (2.41)$$

Hence, from Eq.(2.27), Eq.(2.29), and Eq.(2.41),

$$\begin{aligned}\vec{v}_{1,\hat{z}} &= V_{\hat{Z}} - \frac{m_2 \sin(I)}{m_1 + m_2} (\dot{r} \sin(\omega + f) + r \dot{f} \cos(\omega + f)) \\ &= V_{\hat{Z}} - \frac{m_2 \sin(I)}{m_1 + m_2} \frac{na}{\sqrt{1 - e^2}} (e \sin(f) \sin(\omega + f) + (1 + e \cos(f)) \cos(\omega + f)) \\ &= V_{\hat{Z}} - \frac{m_2 \sin(I)}{m_1 + m_2} C,\end{aligned}\quad (2.42)$$

where



$$C = \frac{na}{\sqrt{1 - e^2}} (e \cos(\omega) + \cos(\omega + f)).\quad (2.43)$$

Similarly, we have the velocity of particle P_2 , and denoted $\vec{v}_{2,\hat{z}}$, that is,

$$\vec{v}_{2,\hat{z}} = V_{\hat{Z}} + \frac{m_1 \sin(I)}{m_1 + m_2} C,\quad (2.44)$$

where C is above in Eq.(2.43).

Suppose that the proper motion of the barycentric velocity is zero, that is, $V_{\hat{Z}} = 0$. Then, from Eq.(2.42) and Eq.(2.44), the value of the radial velocity ratio is

$$\frac{|\vec{v}_{1,\hat{z}}|}{|\vec{v}_{2,\hat{z}}|} = \frac{|V_{\hat{Z}} - \frac{m_2 \sin(I)}{m_1 + m_2} C|}{|V_{\hat{Z}} + \frac{m_1 \sin(I)}{m_1 + m_2} C|} = \frac{\left| -\frac{m_2 \sin(I)}{m_1 + m_2} \right|}{\left| \frac{m_1 \sin(I)}{m_1 + m_2} \right|} = \frac{m_2}{m_1},\quad (2.45)$$

where C is above in Eq.(2.43).

Therefore, from Eq.(2.45), the relation between the observe of orbital radial velocity ratio and the mass ratio of binary system in space is

$$\frac{|\vec{v}_{1,\hat{z}}|}{|\vec{v}_{2,\hat{z}}|} = \frac{m_2}{m_1}.\quad (2.46)$$

Chapter 3

The Orbit Behaviors of Supermassive Binary Black Hole in Galaxical Potential



The purpose of this chapter is to introduce the orbit behavior of the supermassive binary black hole system in a galaxical potential. Firstly, we use the form of galaxical potential in Jiang and Yeh [3] as below :

$$V(r) = -4\pi G \left[\frac{1}{r} \int_0^r \rho(\bar{r}) \bar{r}^2 d\bar{r} + \int_r^\infty \rho(\bar{r}) \bar{r} d\bar{r} \right], \quad (3.1)$$

where G is the universal gravitational constant, r is a radius of the galaxy, and ρ is a density distribution function. Furthermore, which use the Nuker law (Lauer et al. [6] and Jiang and Yeh [3]) as the density distribution function. The Nuker law is expressed below

$$\rho(r) = \rho_c r^{-\gamma} (1 + r^\alpha)^{(\gamma-\beta)/\alpha}, \quad (3.2)$$

where ρ_c , α , β , and γ are constants. Kandrup potential model (Kandrup et al. [4]) was choosing $\alpha = 2$, $\beta = 4$, and $\gamma = 0$. Then the total mass of the galaxy upto a radius r is

$$\begin{aligned} M_g &= 4\pi \int_0^\infty \bar{r}^2 \rho(\bar{r}) d\bar{r} = 4\pi \lim_{r \rightarrow \infty} \int_0^r \bar{r}^2 \rho_c (1 + \bar{r}^2)^{-2} d\bar{r} \\ &= 4\pi \rho_c \lim_{r \rightarrow \infty} \left[\int_0^r \frac{1 + \bar{r}^2}{(1 + \bar{r}^2)^2} d\bar{r} - \int_0^r \frac{1}{(1 + \bar{r}^2)^2} d\bar{r} \right] \\ &= 4\pi \rho_c \lim_{r \rightarrow \infty} \left[\int_0^r \frac{1}{1 + \bar{r}^2} d\bar{r} - \int_0^r \frac{1}{(1 + \bar{r}^2)^2} d\bar{r} \right]. \end{aligned} \quad (3.3)$$

And we use trigonometric substitution to evaluate Eq.(3.3), that is,

$$\begin{aligned} M_g &= 4\pi \rho_c \lim_{r \rightarrow \infty} \left[\int_0^r \frac{1}{1 + \bar{r}^2} d\bar{r} - \int_0^r \frac{1}{(1 + \bar{r}^2)^2} d\bar{r} \right] \\ &= 4\pi \rho_c \lim_{r \rightarrow \infty} \left[\arctan(\bar{r}) - \left(\frac{\bar{r}}{2(1 + \bar{r}^2)} + \frac{\arctan(\bar{r})}{2} \right) \right]_0^r \\ &= 2\pi \rho_c \lim_{r \rightarrow \infty} \left[\arctan(\bar{r}) - \frac{\bar{r}}{1 + \bar{r}^2} \right]_0^r = 2\pi \rho_c \cdot \frac{1}{2}\pi = \pi^2 \rho_c. \end{aligned} \quad (3.4)$$

From Eq.(3.4), we obtain

$$\rho_c = \frac{M_g}{\pi^2}. \quad (3.5)$$

From Eq.(3.1)-(3.2), we could get the potential

$$\begin{aligned} V(r) &= -4\pi G \left[\frac{1}{r} \int_0^r \rho(\bar{r}) \bar{r}^2 d\bar{r} + \int_r^\infty \rho(\bar{r}) \bar{r} d\bar{r} \right] \\ &= -4\pi G \rho_c \left[\frac{1}{r} \int_0^r (1 + \bar{r}^2)^{-2} \bar{r}^2 d\bar{r} + \int_r^\infty (1 + \bar{r}^2)^{-2} \bar{r} d\bar{r} \right]. \end{aligned}$$

Then, we substitute the result of Eq.(3.5) into the above equation. We have

$$V(r) = -\frac{4GM_g}{\pi} \left[\frac{1}{r} \int_0^r (1 + \bar{r}^2)^{-2} \bar{r}^2 d\bar{r} + \int_r^\infty (1 + \bar{r}^2)^{-2} \bar{r} d\bar{r} \right]. \quad (3.6)$$

We use the same process in Eq.(3.3)-(3.4) to solve the first integral in Eq.(3.6). Then

$$\begin{aligned} V(r) &= -\frac{4GM_g}{\pi} \left[\frac{1}{r} \int_0^r (1 + \bar{r}^2)^{-2} \bar{r}^2 d\bar{r} + \int_r^\infty (1 + \bar{r}^2)^{-2} \bar{r} d\bar{r} \right] \\ &= -\frac{4GM_g}{\pi} \left[\left(\frac{\arctan(r)}{2r} - \frac{1}{2(1 + r^2)} \right) + \int_r^\infty (1 + \bar{r}^2)^{-2} \bar{r} d\bar{r} \right]. \end{aligned} \quad (3.7)$$

Moreover, in the second integral in Eq.(3.6), we substitute t for $1 + \bar{r}^2$, then

$$\begin{aligned}
V(r) &= -\frac{4GM_g}{\pi} \left[\left(\frac{\arctan(r)}{2r} - \frac{1}{2(1+r^2)} \right) + \int_r^\infty (1+\bar{r}^2)^{-2} \bar{r} d\bar{r} \right] \\
&= -\frac{4GM_g}{\pi} \left[\left(\frac{\arctan(r)}{2r} - \frac{1}{2(1+r^2)} \right) + \frac{1}{2} \int_{\sqrt{r-1}}^\infty \frac{1}{t^2} dt \right] \\
&= -\frac{4GM_g}{\pi} \left[\left(\frac{\arctan(r)}{2r} - \frac{1}{2(1+r^2)} \right) + \frac{1}{2(1+r^2)} \right] \\
&= -\frac{4GM_g}{\pi} \cdot \frac{\arctan(r)}{2r} \\
&= -c \frac{\arctan r}{r},
\end{aligned} \tag{3.8}$$

where $c = \frac{2}{\pi} GM_g$. From the galactical potential, we get the galactical force as

$$F_g(r) = -\frac{dV}{dr} = c \left[\frac{1}{r(1+r^2)} - \frac{\arctan(r)}{r^2} \right]. \tag{3.9}$$



3.1 Equations of Motion

Suppose that supermassive binary black hole system with a separate distance \bar{r} . Let the location of black holes be \vec{r}_1 , \vec{r}_2 , and let $\bar{r}_i = |\vec{r}_i| = \sqrt{\bar{x}_i^2 + \bar{y}_i^2 + \bar{z}_i^2}$, $i = 1, 2$. Let $\bar{r}_{12} = |\vec{r}_2 - \vec{r}_1| = \sqrt{(\bar{x}_2 - \bar{x}_1)^2 + (\bar{y}_2 - \bar{y}_1)^2 + (\bar{z}_2 - \bar{z}_1)^2}$ in three-dimensional space. Let the mass of two black holes be \bar{m}_1 and \bar{m}_2 . Then our system of motion equation with respect to the time \bar{t} could be written as :

$$\begin{cases} \frac{d\bar{x}_i}{d\bar{t}} = \bar{u}_i \\ \frac{d\bar{y}_i}{d\bar{t}} = \bar{v}_i \\ \frac{d\bar{z}_i}{d\bar{t}} = \bar{w}_i \\ \frac{d\bar{u}_i}{d\bar{t}} = -\frac{\bar{\mu}\bar{x}_i}{\bar{r}_{12}^3} + \frac{\partial V(\bar{r}_i)}{\partial \bar{x}_i} \\ \frac{d\bar{v}_i}{d\bar{t}} = -\frac{\bar{\mu}\bar{y}_i}{\bar{r}_{12}^3} + \frac{\partial V(\bar{r}_i)}{\partial \bar{y}_i} \\ \frac{d\bar{w}_i}{d\bar{t}} = -\frac{\bar{\mu}\bar{z}_i}{\bar{r}_{12}^3} + \frac{\partial V(\bar{r}_i)}{\partial \bar{z}_i}, \end{cases} \tag{3.10}$$

where $\bar{\mu} = G(\bar{m}_1 + \bar{m}_2)$ and $i = 1, 2$. From Eq.(3.8), we could rewrite Eq.(3.10) as :

$$\left\{ \begin{array}{l} \frac{d\bar{x}_i}{dt} = \bar{u}_i \\ \frac{d\bar{y}_i}{dt} = \bar{v}_i \\ \frac{d\bar{z}_i}{dt} = \bar{w}_i \\ \frac{d\bar{u}_i}{dt} = -\frac{\bar{\mu}\bar{x}_i}{\bar{r}_{12}^3} + \frac{c\bar{x}_i}{\bar{r}_i} \left[\frac{1}{\bar{r}_i(1+\bar{r}_i^2)} - \frac{\arctan(\bar{r}_i)}{\bar{r}_i^2} \right] \\ \frac{d\bar{v}_i}{dt} = -\frac{\bar{\mu}\bar{y}_i}{\bar{r}_{12}^3} + \frac{c\bar{y}_i}{\bar{r}_i} \left[\frac{1}{\bar{r}_i(1+\bar{r}_i^2)} - \frac{\arctan(\bar{r}_i)}{\bar{r}_i^2} \right] \\ \frac{d\bar{w}_i}{dt} = -\frac{\bar{\mu}\bar{z}_i}{\bar{r}_{12}^3} + \frac{c\bar{z}_i}{\bar{r}_i} \left[\frac{1}{\bar{r}_i(1+\bar{r}_i^2)} - \frac{\arctan(\bar{r}_i)}{\bar{r}_i^2} \right]. \end{array} \right. \quad (3.11)$$

To apply the mathematical models on real physical systems conveniently, we do non-dimensionalization for the above system. Suppose that the units of length, mass, time, and velocity are L_0, m_0, t_0 , and $\Gamma_0 = \frac{L_0}{t_0}$, respectively. Then non-dimensional variables are

$$\begin{aligned} x_i &= \frac{\bar{x}_i}{L_0}, & y_i &= \frac{\bar{y}_i}{L_0}, & z_i &= \frac{\bar{z}_i}{L_0}, & r_i &= \frac{\bar{r}_i}{L_0}, & r_{12} &= \frac{\bar{r}_{12}}{L_0}, \\ t &= \frac{\bar{t}}{t_0}, & u_i &= \frac{\bar{u}_i}{\Gamma_0}, & v_i &= \frac{\bar{v}_i}{\Gamma_0}, & w_i &= \frac{\bar{w}_i}{\Gamma_0}, & m_i &= \frac{\bar{m}_i}{m_0}, \end{aligned}$$

and set $Gm_0 = \frac{L_0^3}{t_0^2}$. Hence, our system could be written as :

$$\left\{ \begin{array}{l} \frac{dx_i}{dt} = u_i \\ \frac{dy_i}{dt} = v_i \\ \frac{dz_i}{dt} = w_i \\ \frac{du_i}{dt} = -\frac{(m_1+m_2)x_i}{r_{12}^3} + \frac{cx_i}{r_i} \left[\frac{1}{r_i(1+r_i^2)} - \frac{\arctan(r_i)}{r_i^2} \right] \\ \frac{dv_i}{dt} = -\frac{(m_1+m_2)y_i}{r_{12}^3} + \frac{cy_i}{r_i} \left[\frac{1}{r_i(1+r_i^2)} - \frac{\arctan(r_i)}{r_i^2} \right] \\ \frac{dw_i}{dt} = -\frac{(m_1+m_2)z_i}{r_{12}^3} + \frac{cz_i}{r_i} \left[\frac{1}{r_i(1+r_i^2)} - \frac{\arctan(r_i)}{r_i^2} \right]. \end{array} \right. \quad (3.12)$$

From System(3.12), we could derive the following equation

$$u_i \frac{du_i}{dt} = \left\{ -\frac{(m_1+m_2)x_i}{r_{12}^3} + \frac{cx_i}{r_i} \left[\frac{1}{r_i(1+r_i^2)} - \frac{\arctan(r_i)}{r_i^2} \right] \right\} \frac{dx_i}{dt}. \quad (3.13)$$

Next, we integrate Eq.(3.13). Then

$$\int \frac{dx_i}{dt} \frac{d^2x_i}{dt^2} dt = \int \left\{ -\frac{(m_1 + m_2)x_i}{r_{12}^3} + \frac{cx_i}{r_i} \left[\frac{1}{r_i(1+r_i^2)} - \frac{\arctan(r_i)}{r_i^2} \right] \right\} \frac{dx_i}{dt} dt. \quad (3.14)$$

Moreover, we obtain

$$\frac{1}{2} \left(\frac{dx_i}{dt} \right)^2 = \int \left\{ -\frac{(m_1 + m_2)x_i}{r_{12}^3} + \frac{cx_i}{r_i} \left[\frac{1}{r_i(1+r_i^2)} - \frac{\arctan(r_i)}{r_i^2} \right] \right\} dx_i. \quad (3.15)$$

In addition, we can have

$$\frac{1}{2} \left(\frac{dy_i}{dt} \right)^2 = \int \left\{ -\frac{(m_1 + m_2)y_i}{r_{12}^3} + \frac{cy_i}{r_i} \left[\frac{1}{r_i(1+r_i^2)} - \frac{\arctan(r_i)}{r_i^2} \right] \right\} dy_i, \quad (3.16)$$

and

$$\frac{1}{2} \left(\frac{dz_i}{dt} \right)^2 = \int \left\{ -\frac{(m_1 + m_2)z_i}{r_{12}^3} + \frac{cz_i}{r_i} \left[\frac{1}{r_i(1+r_i^2)} - \frac{\arctan(r_i)}{r_i^2} \right] \right\} dz_i. \quad (3.17)$$

From Eq.(3.15), Eq.(3.16), and Eq.(3.17), we get

$$\begin{aligned} \frac{1}{2} \left[\left(\frac{dx_i}{dt} \right)^2 + \left(\frac{dy_i}{dt} \right)^2 + \left(\frac{dz_i}{dt} \right)^2 \right] &= \int -\frac{(m_1 + m_2)}{r_{12}^3} (x_i dx_i + y_i dy_i + z_i dz_i) \\ &\quad + c \int \frac{1}{r_i} \left[\frac{1}{r_i(1+r_i^2)} - \frac{\arctan(r_i)}{r_i^2} \right] (x_i dx_i + y_i dy_i + z_i dz_i). \end{aligned}$$

Since $r_i dr_i = x_i dx_i + y_i dy_i + z_i dz_i$,

$$\begin{aligned} \frac{1}{2} \left[\left(\frac{dx_i}{dt} \right)^2 + \left(\frac{dy_i}{dt} \right)^2 + \left(\frac{dz_i}{dt} \right)^2 \right] &= -(m_1 + m_2) \int \frac{r_i}{r_{12}^3} dr_i \\ &\quad + c \int \left[\frac{1}{r_i(1+r_i^2)} - \frac{\arctan(r_i)}{r_i^2} \right] dr_i. \end{aligned} \quad (3.18)$$

Since $r_{12} = r_i(m_1 + m_2)/m_j$, $i \neq j$ and $i, j \in \{1, 2\}$, the first integral on the right hand side of Eq.(3.18) is

$$\begin{aligned}
-(m_1 + m_2) \int \frac{r_i}{r_{12}^3} dr_i &= -(m_1 + m_2) \int \frac{r_i}{\left[\frac{r_i(m_1+m_2)}{m_j} \right]^3} dr_i \\
&= -\frac{m_j^3}{(m_1 + m_2)^2} \int \frac{1}{r_i^2} dr_i = \frac{m_j^3}{r_i(m_1 + m_2)^2} + C_0, \forall C_0 \in \mathbf{R}.
\end{aligned} \tag{3.19}$$

Furthermore, by Eq.(3.8) and Eq.(3.9), the second integral on the right hand side of Eq.(3.18) is

$$c \int \left[\frac{1}{r_i(1+r_i^2)} - \frac{\arctan(r_i)}{r_i^2} \right] dr_i = c \frac{\arctan(r_i)}{r_i} + C_1, \forall C_1 \in \mathbf{R}. \tag{3.20}$$

Hence, using Eq.(3.19) and Eq.(3.20), we rewrite Eq.(3.18) to be

$$\frac{1}{2} \left[\left(\frac{dx_i}{dt} \right)^2 + \left(\frac{dy_i}{dt} \right)^2 + \left(\frac{dz_i}{dt} \right)^2 \right] = \frac{m_j^3}{r_i(m_1 + m_2)^2} + c \frac{\arctan(r_i)}{r_i} + C_i, C_i = C_0 + C_1. \tag{3.21}$$

From System(3.12), we obtain

$$\frac{1}{2} (u_i^2 + v_i^2 + w_i^2) = \frac{m_j^3}{r_i(m_1 + m_2)^2} + c \frac{\arctan(r_i)}{r_i} + C_i. \tag{3.22}$$

Let

$$E_i = \frac{1}{2} (u_i^2 + v_i^2 + w_i^2) - \frac{m_j^3}{r_i(m_1 + m_2)^2} - c \frac{\arctan(r_i)}{r_i}, \tag{3.23}$$

where $i \neq j$, and $i, j \in \{1, 2\}$. Then we define the total energy E_{total} to be

$$E_{total} = E_1 + E_2 = C_J, \forall C_J \in \mathbf{R}. \tag{3.24}$$

3.2 $\mathbf{c} = \mathbf{0}$ Case with a circular orbit

In this section, we will discuss the case of circular orbits under the influence of galactical potential, by controlling the initial energies of the system. First of all, we let $m_1 = m_2 = 0.5$, and $\vec{r}_1(0) = (1, 0, 0)$, $\vec{r}_2(0) = (-1, 0, 0)$ at initial time. Additionally, by Appendix B, let $\omega = \frac{\pi}{6}$, $I = \frac{\pi}{4}$, and $\Omega = \frac{\pi}{6}$, rotate the orbital plane in three-dimensional space. Moreover, from Eq.(3.23), we obtain

$$(u_i^2 + v_i^2 + w_i^2) = 2E_i + \frac{2m_j^3}{r_i(m_1+m_2)^2} + c\frac{2\arctan(r_i)}{r_i} \geq 0. \quad (3.25)$$

Suppose that $U_i = \frac{2m_j^3}{r_i(m_1+m_2)^2} + c\frac{2\arctan(r_i)}{r_i}$. Then we get

$$(u_i^2 + v_i^2 + w_i^2) = 2E_i + U_i \geq 0. \quad (3.26)$$

Hence,

$$E_i \geq -\frac{U_i}{2}. \quad (3.27)$$

In this subsection, we let $c = 0$ and the initial velocity $(u_1(0), v_1(0), w_1(0)) = (0, \sqrt{\frac{Gm_2}{r_1}}, 0) = (0, \sqrt{0.5}, 0)$, $(u_2(0), v_2(0), w_2(0)) = (0, -\sqrt{\frac{Gm_1}{r_2}}, 0) = (0, -\sqrt{0.5}, 0)$. After rotation, the initial positions of P_1 and P_2 are $\vec{r}_1(0) = (0.5732, 0.7392, 0.3563)$ and $\vec{r}_2(0) = (-0.5732, -0.7392, -0.3563)$.

From Figure 3.1, the total energy remains approximately constant 0 from $t = 0$ to $t = 100$ so we know that the system for case $c = 0$ is a conservative system. In Figure 3.2a and Figure 3.2b, we plot the orbits on $\hat{X}\hat{Y}$ -plane and $\hat{X}\hat{Z}$ -plane, respectively. Furthermore, we show the length of r_{12} from $t = 0$ to $t = 100$ in Figure 3.2c. Conclusively, from Figure 3.2d, by plotting the values of orbital radial velocity ratio in \hat{Z} direction from $t = 0$ to $t = 100$, we could know the relation between the orbital radial velocity ratio in \hat{Z} direction and the mass ratio, m_2/m_1 , satisfies Eq.(2.46).

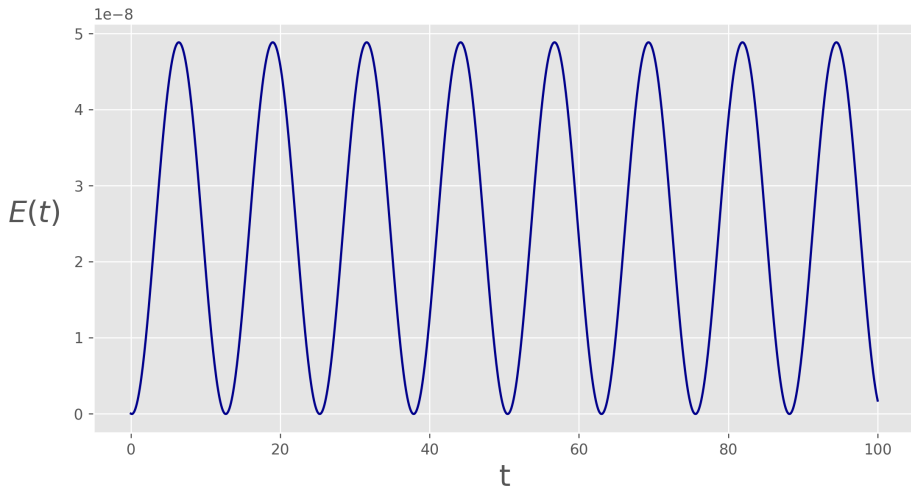


Figure 3.1: The total energy from $t = 0$ to $t = 100$.

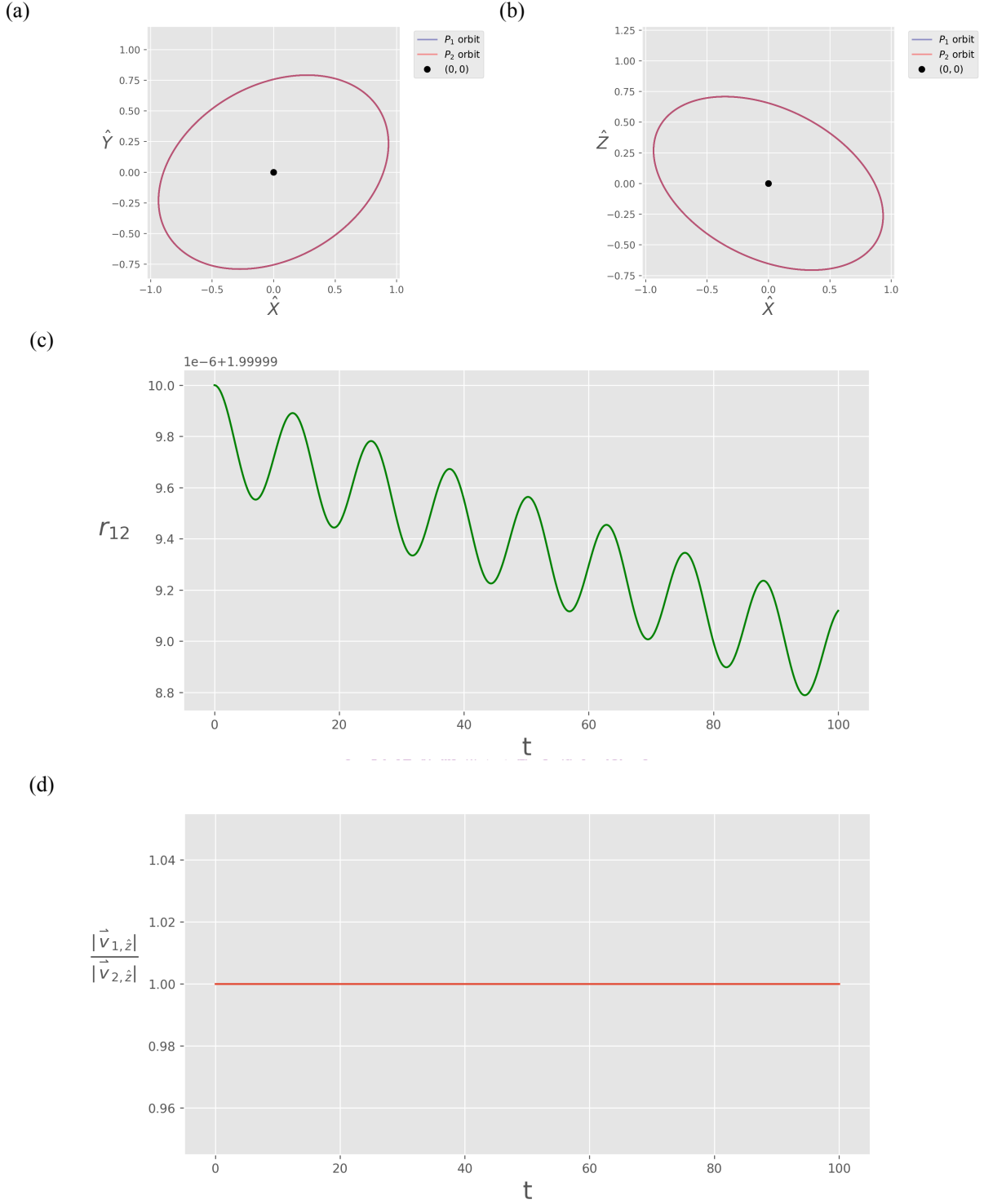


Figure 3.2: Case of $c = 0$. (a) The orbit on $\hat{X}\hat{Y}$ -plane from $t = 0$ to $t = 100$. (b) The orbit on $\hat{X}\hat{Z}$ -plane from $t = 0$ to $t = 100$. (c) The length of r_{12} from $t = 0$ to $t = 100$. (d) The orbital radial velocity ratio from $t = 0$ to $t = 100$.

3.3 $\mathbf{c} \neq \mathbf{0}$ Case with elliptical orbits

In this subsection, we let $c = \frac{2}{\pi} M_g$ and $M_g = \frac{(m_1+m_2)}{2} \cdot 100$ (Milosavljević, M., & Merritt, D. [7]). Additionally, from Eq.(3.26), we let $E_{total}^c = 2U_i$ with $m_1 = m_2 = 0.5$, i.e.

$$E_{total}^c = 2U_i = 0.5 + 4c \arctan(1). \quad (3.28)$$

Then we choose different mass assumptions to represent various models and discuss the relation between the orbital radial velocity ratio and the mass ratio under different initial total energy conditions, E_0 . Moreover, by Eq.(3.26), the initial velocity, $V_i^2(0) = u_i^2(0) + v_i^2(0) + w_i^2(0) = -\frac{1}{2}E_0$.

3.3.1 Equal mass case

In this subsection, we suppose that $m_1 = m_2 = 0.5$. We choose initial total energy $E_0 = -E_{total}^c/2$ for Model A1 and $E_0 = -E_{total}^c/18$ for Model A2. Then we find the initial velocity $V_i^2(0) = \frac{1}{4}E_{total}^c = 12.5625$ and $V_i^2(0) = \frac{1}{36}E_{total}^c = 1.3958$ for Model A1 and Model A2, respectively. After rotation, the initial positions of P_1 and P_2 are $\vec{r}_1(0) = (0.5732, 0.7392, 0.3563)$ and $\vec{r}_2(0) = (-0.5732, -0.7392, -0.3563)$.

From Figure 3.3a, Figure 3.3b, and Figure 3.4, we know that Model A1 orbits are periodically elliptical orbits. Moreover, we can see that in Model A2, the distance between the two particles gradually becomes shorter, from Figure 3.3c, Figure 3.3d, and Figure 3.4. Additionally, we obtain the orbital radial velocity ratio $|\vec{v}_{1,\hat{z}}|/|\vec{v}_{2,\hat{z}}| = 1 = m_2/m_1$ for those two models, which satisfies the Eq.(2.46).

Model	E_0	$V_i^2(0)$	maximum $v_{1,\hat{z}} / v_{2,\hat{z} }$	minimum $v_{1,\hat{z}} / v_{2,\hat{z} }$
Model A1	-25.1250	12.5625	1.0000	1.0000
Model A2	-2.7917	1.3958	1.0000	1.0000

Table 3.1: Model with $m_1 = m_2 = 0.5$.

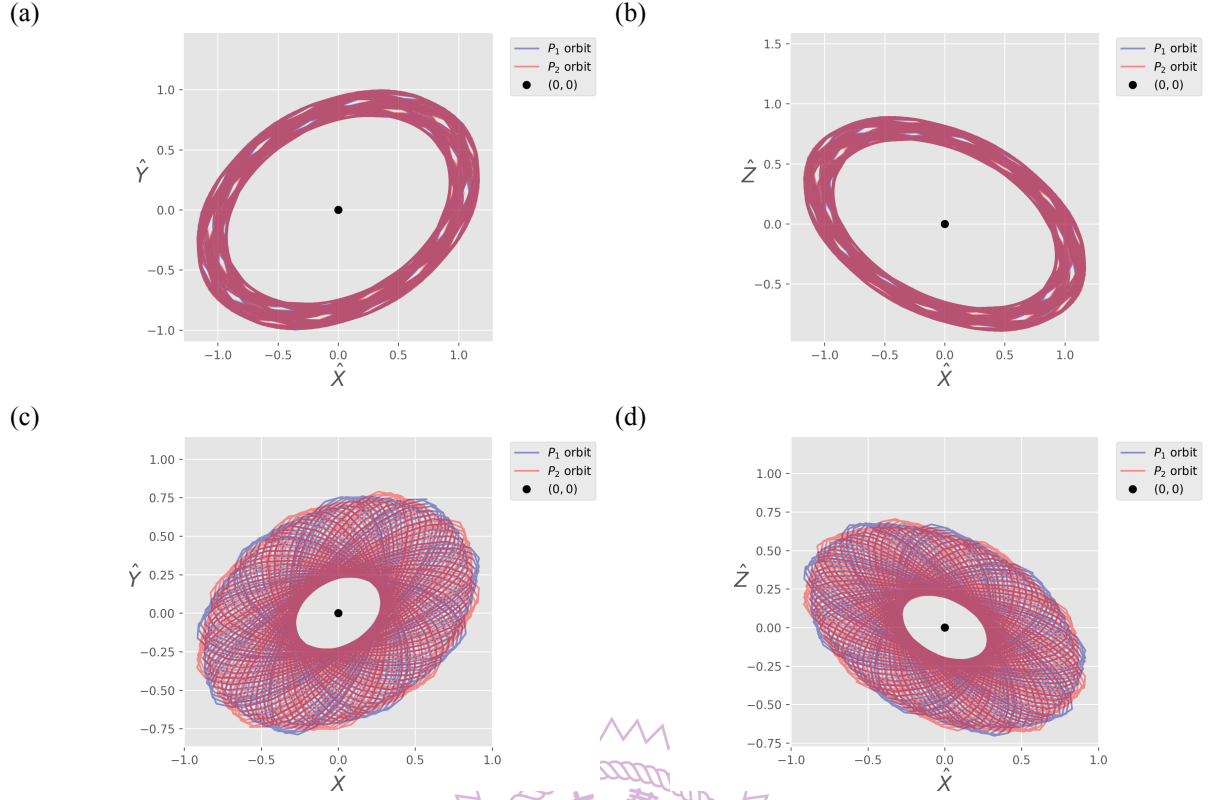


Figure 3.3: Orbital plots of Model A1 and Model A2. (a) The Model A1 orbit on $\hat{X}\hat{Y}$ -plane from $t = 0$ to $t = 100$. (b) The Model A1 orbit on $\hat{X}\hat{Z}$ -plane from $t = 0$ to $t = 100$. (c) The Model A2 orbit on $\hat{X}\hat{Y}$ -plane from $t = 0$ to $t = 100$. (d) The Model A2 orbit on $\hat{X}\hat{Z}$ -plane from $t = 0$ to $t = 100$.

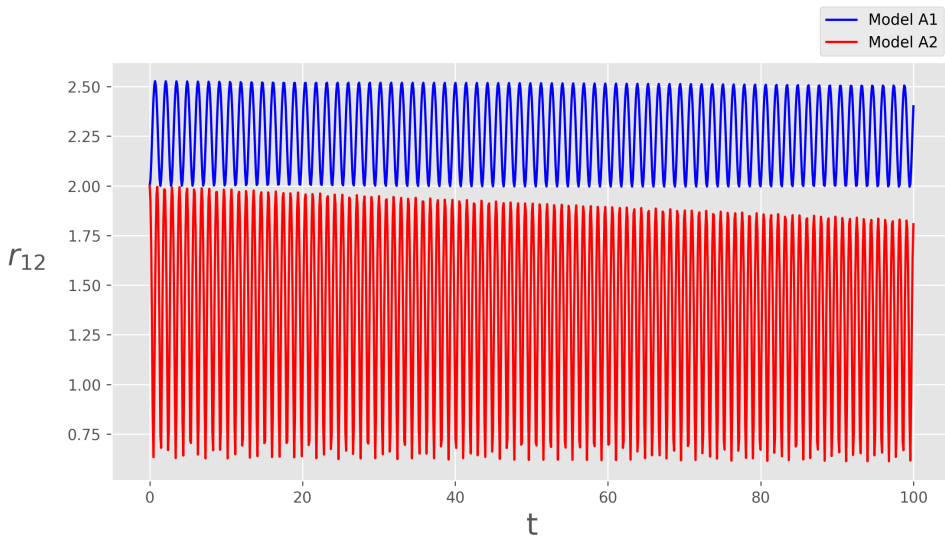


Figure 3.4: The length of r_{12} from $t = 0$ to $t = 100$.

3.3.2 Unequal masses cases

In this subsection, we suppose $m_1 = \alpha$ and $m_2 = 1 - \alpha$. Let the positions of two particles P_1, P_2 are $(1 - \alpha, 0, 0), (-\alpha, 0, 0)$. Furthermore, by Appendix B, let $\omega = \frac{\pi}{6}$, $I = \frac{\pi}{4}$, and $\Omega = \frac{\pi}{6}$, rotate the orbital plane in three-dimensional space.

In Model B1 and Model B2, we choose initial total energy $E_0 = -E_{total}^c/2$ and $E_0 = -E_{total}^c/18$, respectively. Let $\alpha = 0.4$ for Model B1 and Model B2. After rotation, the initial positions of two particles P_1, P_2 are $\vec{r}_1(0) = (0.6879, 0.8870, 0.4243)$, and $\vec{r}_2(0) = (-0.4586, -0.5914, -0.2828)$. From Figure 3.5, we plot the orbits on $\hat{X}\hat{Y}$ -plane and $\hat{X}\hat{Z}$ -plane. Moreover, we show the length of r_{12} for Model B1 and Model B2 in Figure 3.6. According to Figure 3.5a, Figure 3.5b, and Figure 3.6, the orbits are periodically elliptical orbits for Model B1. Otherwise, from Figure 3.5c, Figure 3.5d, and Figure 3.6, the distance between the two particles gradually becomes shorter in Model B2. Eventually, from Figure 3.7, we get the orbital radial velocity ratio $|\vec{v}_{1,\hat{z}}|/|\vec{v}_{2,\hat{z}}| \approx 1.5 = m_2/m_1$, which satisfies the Eq.(2.46).

In Model C1 and Model C2, we set initial total energy $E_0 = -E_{total}^c/2$ and $E_0 = -E_{total}^c/18$, respectively. Let $\alpha = 0.3$ for Model C1 and Model C2. After rotation, the initial positions of two particles P_1, P_2 are $\vec{r}_1(0) = (0.8025, 1.0349, 0.4950)$, $\vec{r}_2(0) = (-0.3439, -0.4435, -0.2121)$. Following Figure 3.8, we plot the orbits on $\hat{X}\hat{Y}$ -plane and $\hat{X}\hat{Z}$ -plane. Furthermore, we display the length of r_{12} for Model C1 and Model C2 in Figure 3.9. Based on Figure 3.8a, Figure 3.8b, and Figure 3.9, the orbits are periodically elliptical orbits for Model C1. Alternatively, from Figure 3.8c, Figure 3.8d, and Figure 3.9, the distance between the two particles gradually becomes shorter in Model C2. Ultimately, from Figure 3.7, we get the orbital radial velocity ratio $|\vec{v}_{1,\hat{z}}|/|\vec{v}_{2,\hat{z}}| \approx 2.3333 \approx 7/3 = m_2/m_1$, which satisfies the Eq.(2.46).

In Model D1 and Model D2, we assume initial total energy $E_0 = -E_{total}^c/2$ and $E_0 = -E_{total}^c/18$, respectively. Let $\alpha = 0.2$ for Model D1 and Model D2. After rotation, the initial positions of two particles P_1, P_2 are $\vec{r}_1(0) = (0.9172, 1.1827, 0.5657)$, and $\vec{r}_2(0) = (-0.2293, -0.2957, -0.1414)$. By Figure 3.11, we plot the orbits on $\hat{X}\hat{Y}$ -plane and $\hat{X}\hat{Z}$ -plane. In addition, we show the length of r_{12} for Model D1 and Model D2 in Figure 3.12. From Figure 3.11a, Figure 3.11b, and Figure 3.12, the orbits are periodically elliptical orbits for Model D1. In another way, from Figure 3.11c, Figure 3.11d, and Figure 3.12, the distance between the two

particles gradually becomes shorter in Model D2. Finally, from Figure 3.13, we get the orbital radial velocity ratio $|\vec{v}_{1,\hat{z}}|/|\vec{v}_{2,\hat{z}}| \approx 4.0 = m_2/m_1$, which satisfies the Eq.(2.46).

Therefore, we present six models in Table 3.2 for different masses α and initial energies.

Model	α	\mathbf{E}_0	$\mathbf{V}_i^2(\mathbf{0})$	maximum $ v_{1,\hat{z}} / v_{2,\hat{z}} $	minimum $ v_{1,\hat{z}} / v_{2,\hat{z}} $
B1	0.4	-25.1250	12.5625	$1.5 + 6.3283 \cdot 10^{-14}$	$1.5 - 7.6161 \cdot 10^{-14}$
B2		-2.7917	1.3958	$1.5 + 7.8826 \cdot 10^{-14}$	$1.5 - 1.7675 \cdot 10^{-13}$
C1	0.3	-25.1250	12.5625	$2.3333 + 2.0295 \cdot 10^{-13}$	$2.3333 - 8.8374 \cdot 10^{-14}$
C2		-2.7917	1.3958	$2.3333 + 1.5676 \cdot 10^{-13}$	$2.3333 - 7.0166 \cdot 10^{-14}$
D1	0.2	-25.1250	12.5625	$4.0 + 4.4942 \cdot 10^{-13}$	$4.0 - 6.0885 \cdot 10^{-13}$
D2		-2.7917	1.3958	$4.0 + 2.8244 \cdot 10^{-13}$	$4.0 - 1.4033 \cdot 10^{-13}$

Table 3.2: Models with $m_1 = \alpha$, $m_2 = 1 - \alpha$.

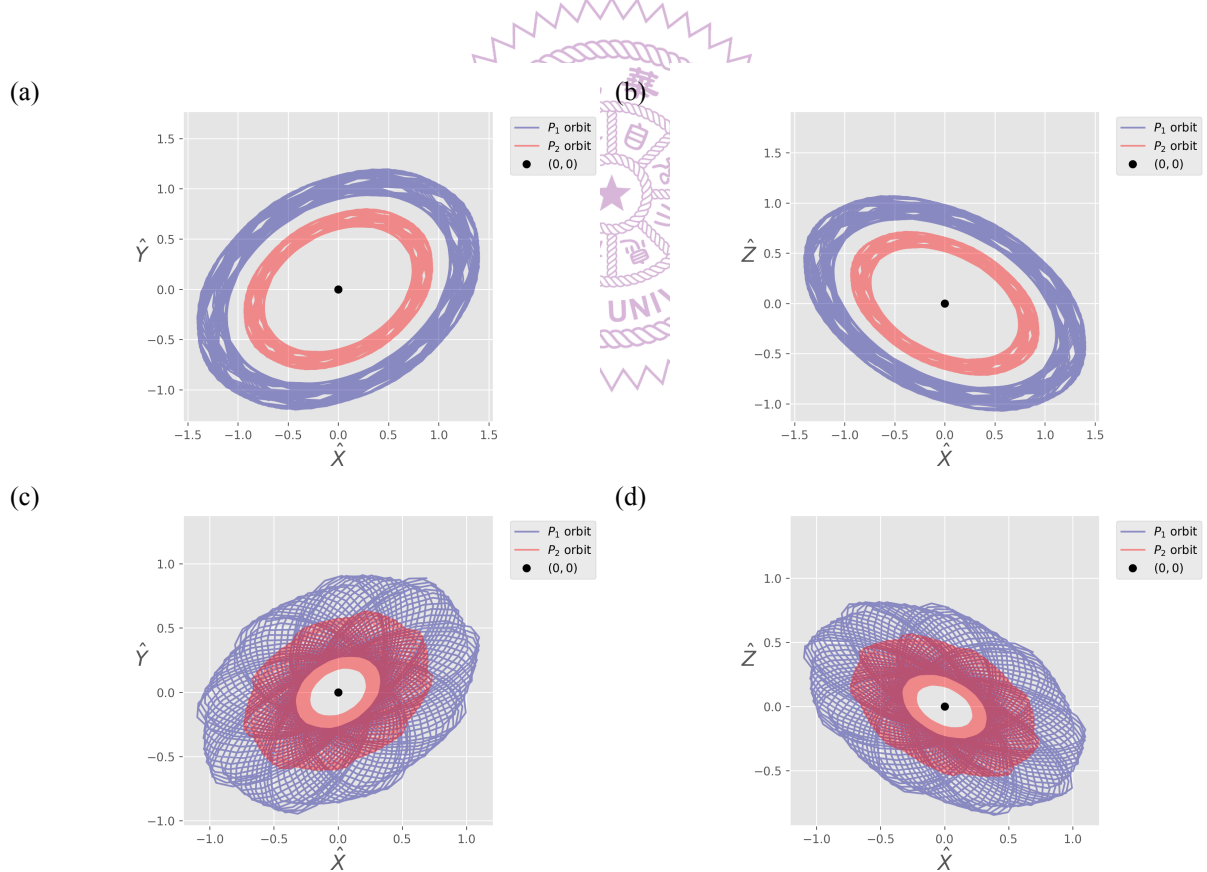


Figure 3.5: Orbital plots of Model B1 and Model B2. (a) The Model B1 orbit on $\hat{X}\hat{Y}$ -plane from $t = 0$ to $t = 100$. (b) The Model B1 orbit on $\hat{X}\hat{Z}$ -plane from $t = 0$ to $t = 100$. (c) The Model B2 orbit on $\hat{X}\hat{Y}$ -plane from $t = 0$ to $t = 100$. (d) The Model B2 orbit on $\hat{X}\hat{Z}$ -plane from $t = 0$ to $t = 100$.

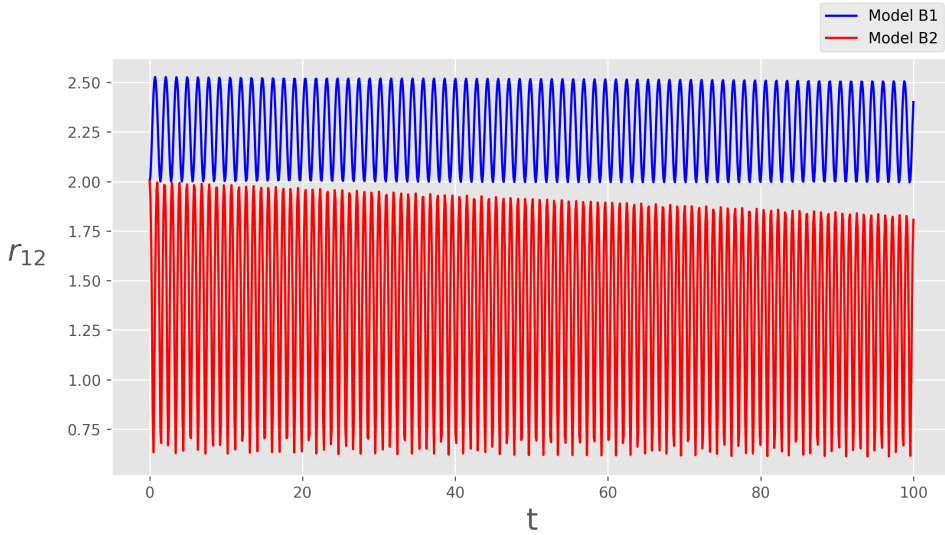


Figure 3.6: The length of r_{12} from $t = 0$ to $t = 100$.

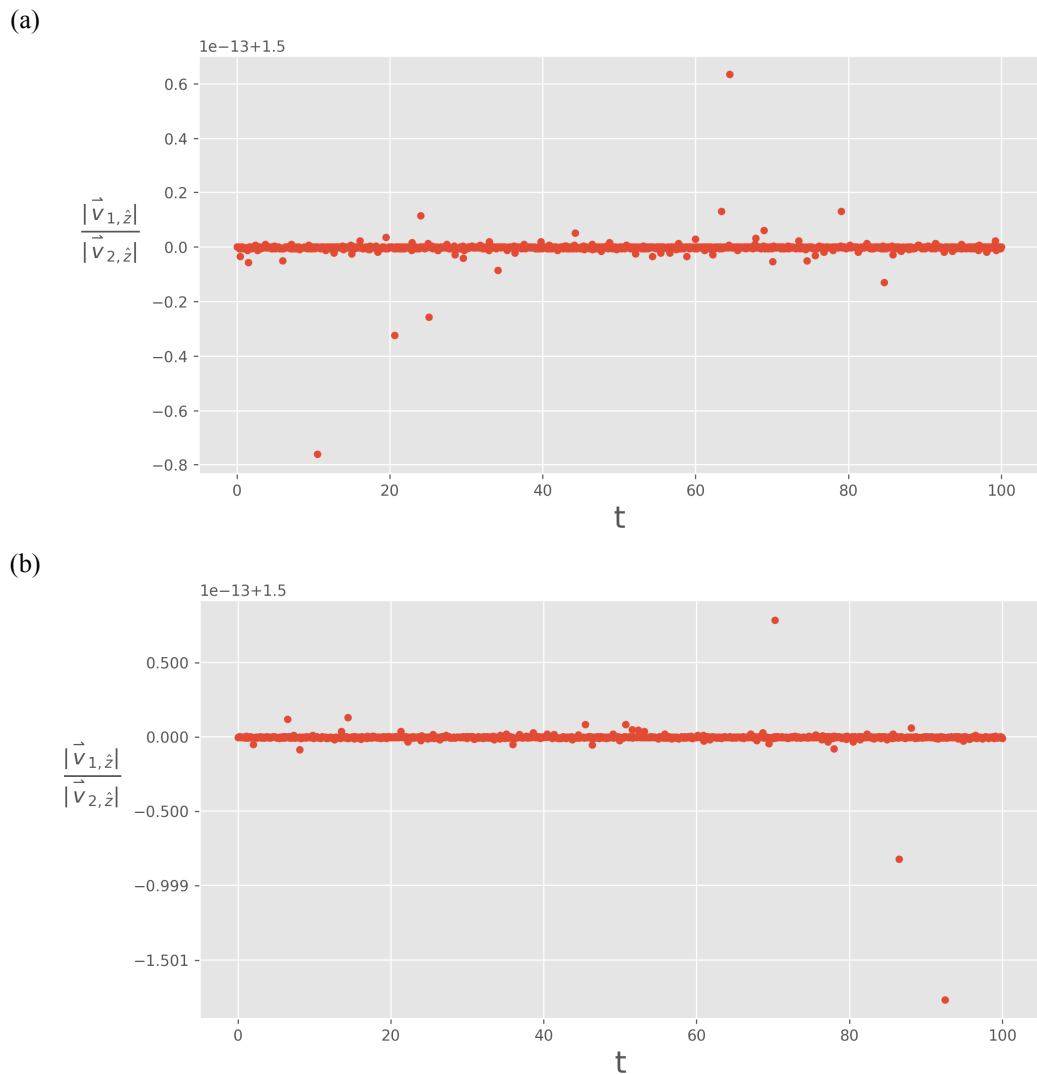


Figure 3.7: The orbital radial velocity ratio from $t = 0$ to $t = 100$. (a) The Model B1. (b) The Model B2.

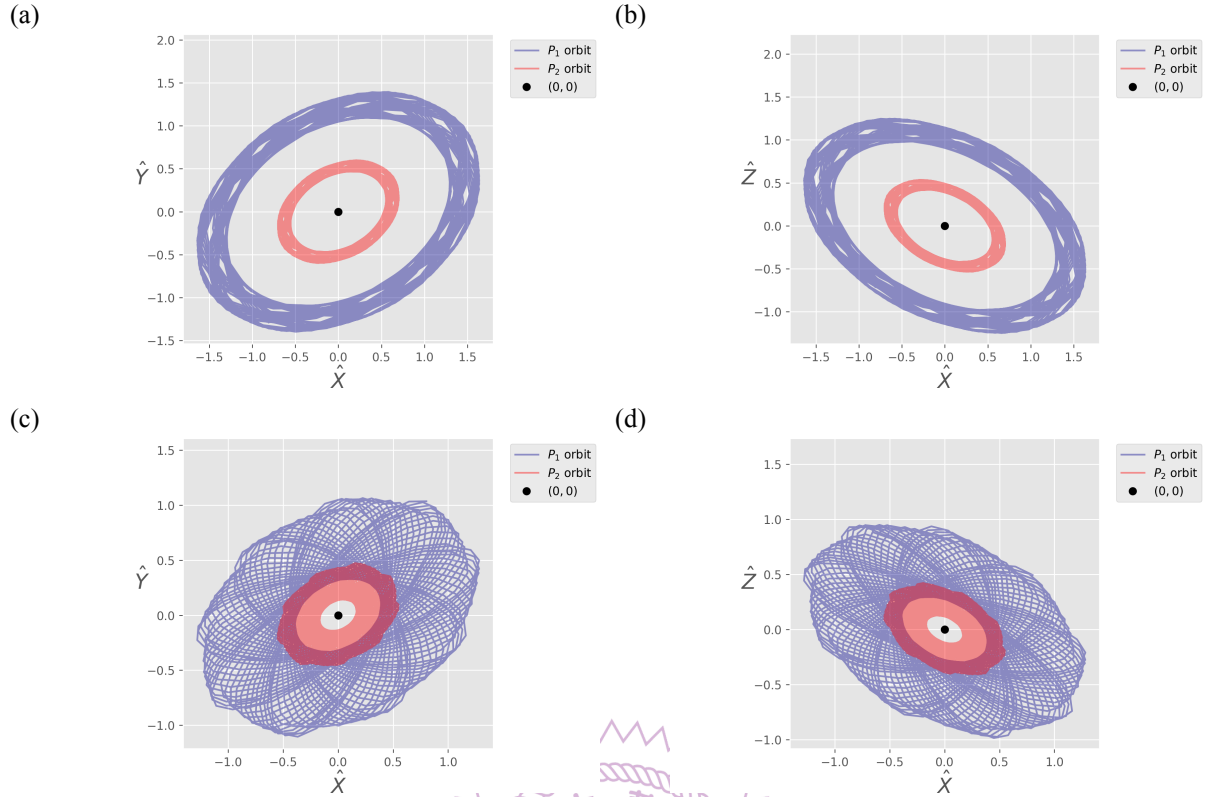


Figure 3.8: Orbital plots of Model C1 and Model C2. (a) The Model C1 orbit on $\hat{X}\hat{Y}$ -plane from $t = 0$ to $t = 100$. (b) The Model C1 orbit on $\hat{X}\hat{Z}$ -plane from $t = 0$ to $t = 100$. (c) The Model C2 orbit on $\hat{X}\hat{Y}$ -plane from $t = 0$ to $t = 100$. (d) The Model C2 orbit on $\hat{X}\hat{Z}$ -plane from $t = 0$ to $t = 100$.

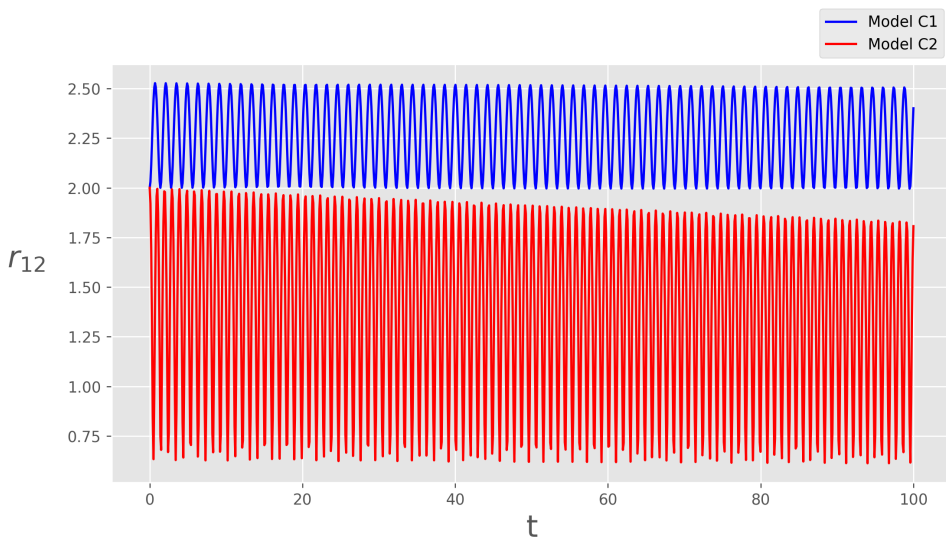


Figure 3.9: The length of r_{12} from $t = 0$ to $t = 100$.

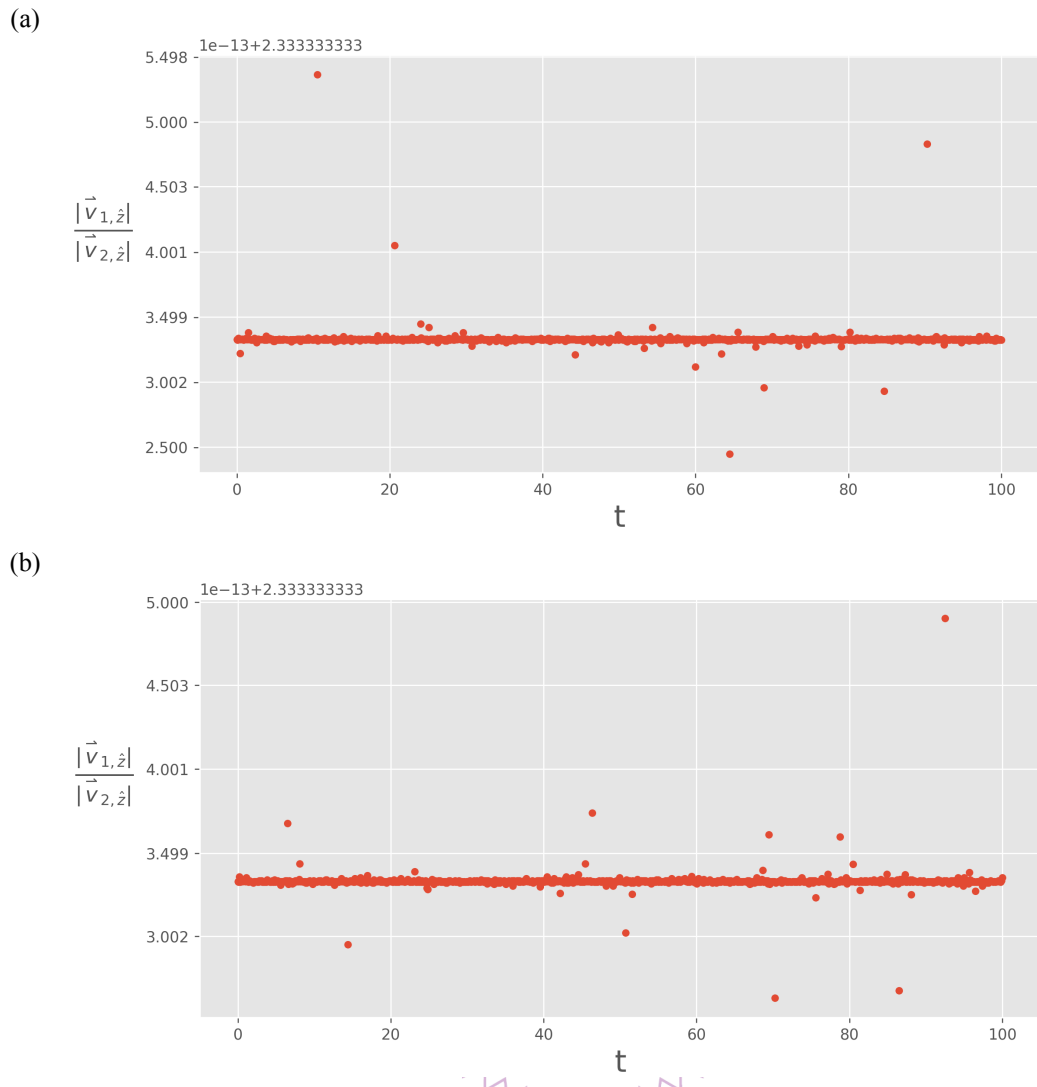


Figure 3.10: The orbital radial velocity ratio from $t = 0$ to $t = 100$. (a) The Model C1. (b) The Model C2.

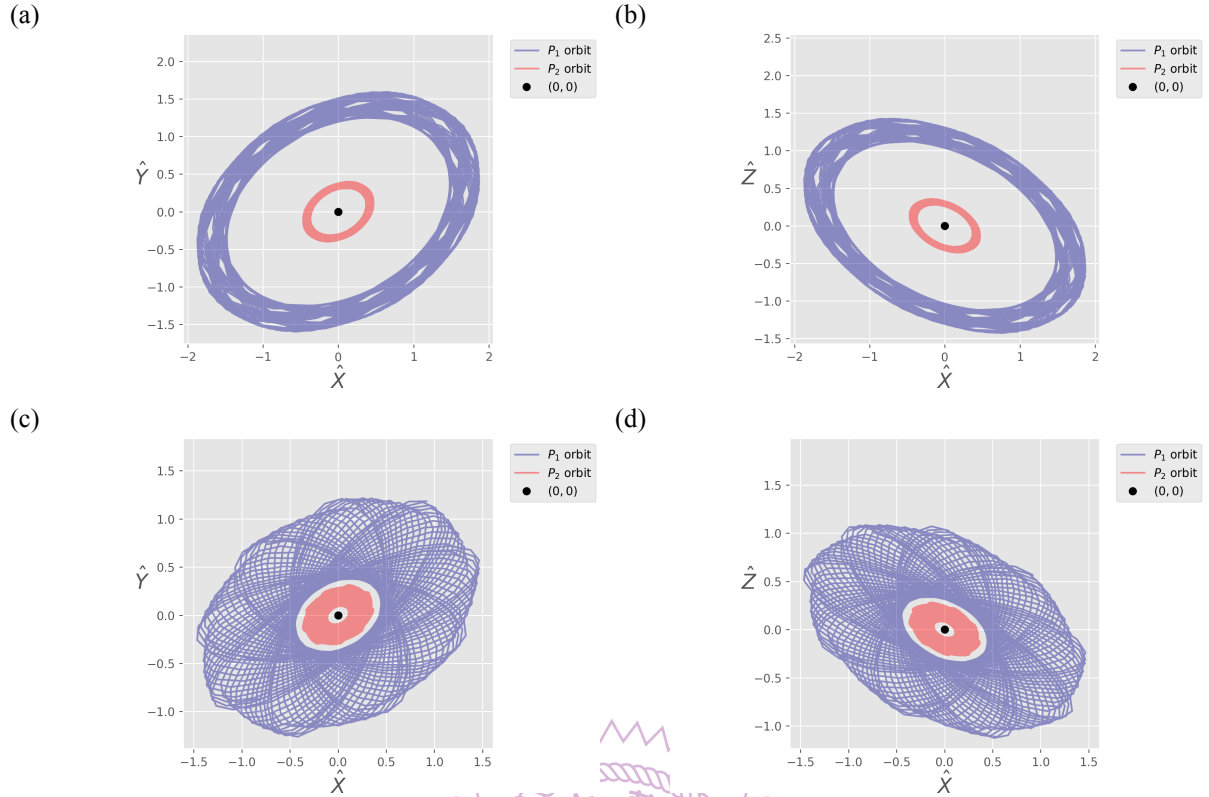


Figure 3.11: Orbital plots of Model D1 and Model D2. (a) The Model D1 orbit on $\hat{X}\hat{Y}$ -plane from $t = 0$ to $t = 100$. (b) The Model D1 orbit on $\hat{X}\hat{Z}$ -plane from $t = 0$ to $t = 100$. (c) The Model D2 orbit on $\hat{X}\hat{Y}$ -plane from $t = 0$ to $t = 100$. (d) The Model D2 orbit on $\hat{X}\hat{Z}$ -plane from $t = 0$ to $t = 100$.

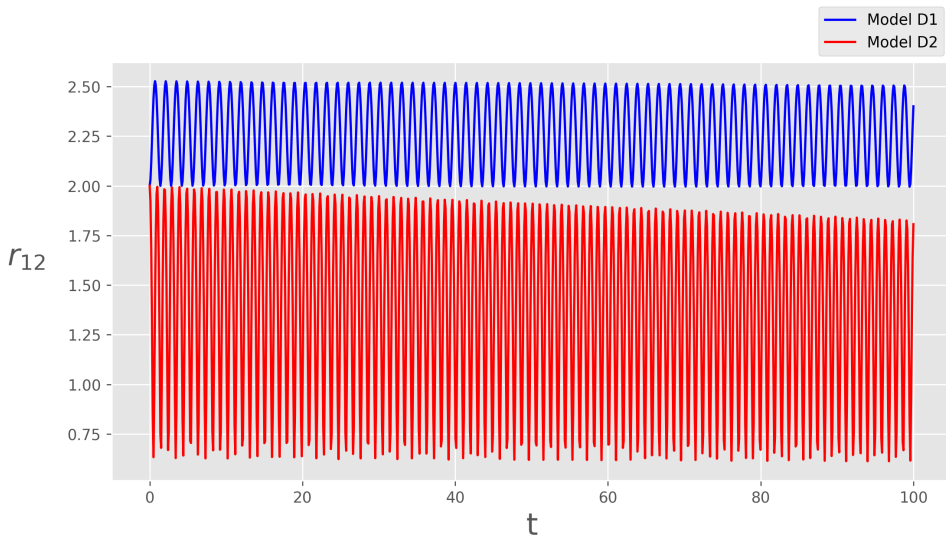


Figure 3.12: The length of r_{12} from $t = 0$ to $t = 100$.

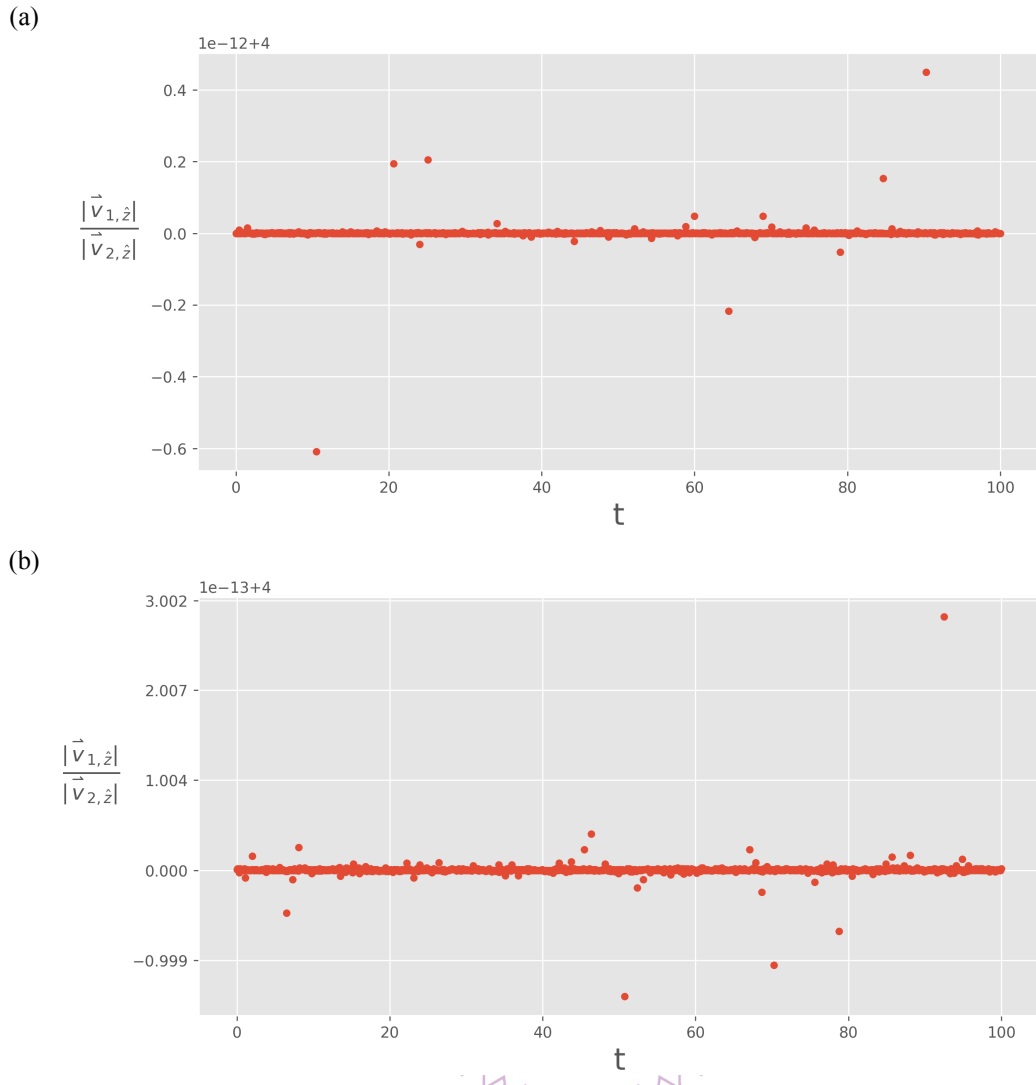


Figure 3.13: The orbital radial velocity ratio from $t = 0$ to $t = 100$. (a) The Model D1. (b) The Model D2.

3.3.3 Different total mass of galaxy

In this subsection, we suppose different total mass of the galaxy assumption, i.e.,

$$M_g = \frac{(m_1 + m_2)}{2} \cdot \kappa. \quad (3.29)$$

In section 3.3, we choose $\kappa = 100$. Then, in this subsection, we choose different value of κ .

Firstly, we calculate and plot $V(r)$ for different values of κ (see Figure 3.14).

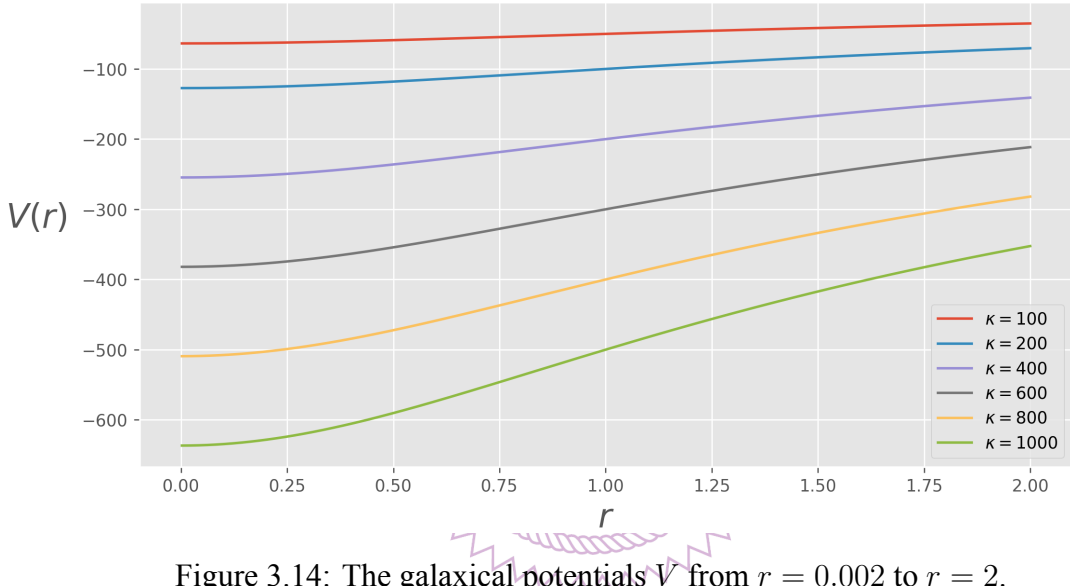


Figure 3.14: The galactical potentials V from $r = 0.002$ to $r = 2$.

We choose $\kappa = 1000$ to observe the effects of orbital radial velocity ratio in different mass case. Then, from Eq.(3.29), $M_g = \frac{(m_1+m_2)}{2} \cdot 1000$. Let $m_1 = 0.2$ and $m_2 = 0.8$. Let the positions of two particles P_1, P_2 are $(0.8, 0, 0)$, $(-0.2, 0, 0)$. Moreover, by Appendix B, let $\omega = \frac{\pi}{6}$, $I = \frac{\pi}{4}$, and $\Omega = \frac{\pi}{6}$, rotate the orbital plane in three-dimensional space.

We assume initial total energy $E_0 = -E_{total}^c/2$. After rotation, the initial positions of two particles P_1, P_2 are $\vec{r}_1(0) = (0.9172, 1.1827, 0.5657)$, and $\vec{r}_2(0) = (-0.2293, -0.2957, -0.1414)$. From Figure 3.15, the maximum value of $|\vec{v}_{1,\hat{z}}|/|\vec{v}_{2,\hat{z}}|$ is $4.0 + 2.5544 \cdot 10^{-12}$ and the minimum value of $|\vec{v}_{1,\hat{z}}|/|\vec{v}_{2,\hat{z}}|$ is $4.0 - 7.7023 \cdot 10^{-12}$. We obtain the orbital radial velocity ratio $|\vec{v}_{1,\hat{z}}|/|\vec{v}_{2,\hat{z}}| \approx 4.0 = m_2/m_1$.

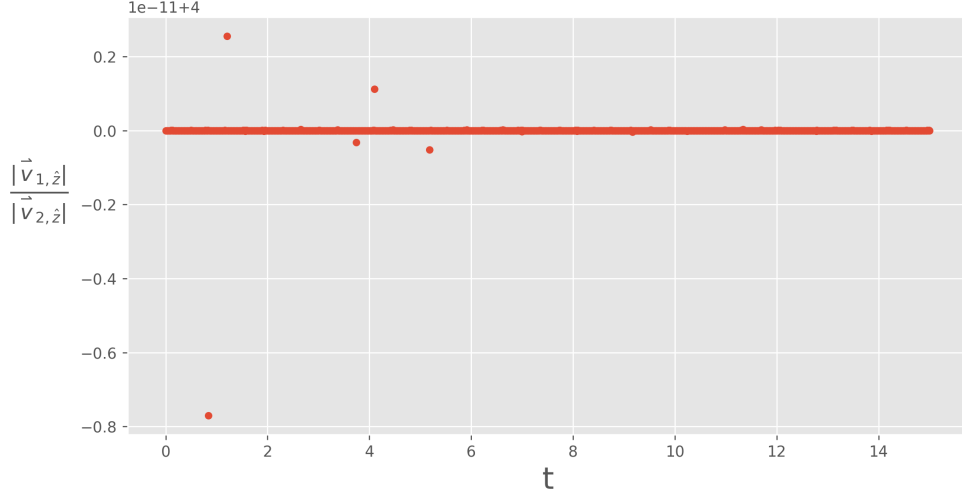


Figure 3.15: The orbital radial velocity ratio with $E_0 = -E_{total}^c/2$ from $t = 0$ to $t = 15$.

Furthermore, we assume initial total energy $E_0 = -E_{total}^c/18$. After rotation, the initial positions of two particles P_1, P_2 are $\vec{r}_1(0) = (0.9172, 1.1827, 0.5657)$, and $\vec{r}_2(0) = (-0.2293, -0.2957, -0.1414)$. From Figure 3.16, , the maximum value of $|\vec{v}_{1,\hat{z}}|/|\vec{v}_{2,\hat{z}}|$ is $4.0 + 8.4377 \cdot 10^{-14}$ and the minimum value of $|\vec{v}_{1,\hat{z}}|/|\vec{v}_{2,\hat{z}}|$ is $4.0 - 1.0436 \cdot 10^{-13}$. We get the orbital radial velocity ratio $|\vec{v}_{1,\hat{z}}|/|\vec{v}_{2,\hat{z}}| \approx 4.0 = m_2/m_1$.

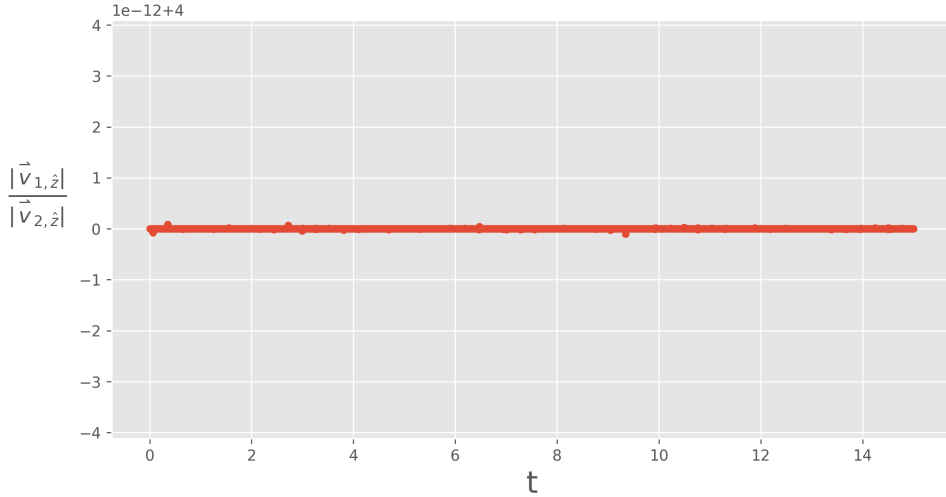


Figure 3.16: The orbital radial velocity ratio with $E_0 = -E_{total}^c/18$ from $t = 0$ to $t = 15$.

Therefore, we can know that the result remain unchanged for larger values of parameter κ . The relation between the velocity ratio and mass ratio is an inverse proportionality.

Chapter 4

Conclusion

This study focuses on investigating the correlation between the velocity ratio and mass ratio in the binary black holes within the galactic potential.

In Chapter 2, we analyse the equation of motion of the two-body problem in circular and elliptical orbits separately and discuss the relation between velocity ratio and mass ratio. Our observations reveal an inverse relationship between the mass ratio and velocity ratio.

Subsequently, in Chapter 3, we explore the results of relationship between the mass ratio and velocity ratio in the galactic potential. By considering different particle masses and initial total energies, we present that the mass ratio of the two particles exhibits an inverse proportionality to the velocity ratio. Moreover, we choose larger mass of galaxy for different particle masses and initial total energies. Then result also show that the relation between the velocity ratio and mass ratio is an inverse proportionality.

Based on the numerical computations, it can be inferred that within the binary black holes model under the galactic potential. Furthermore, an inverse correlation between the mass ratio and velocity ratio is observed for several different masses and total energy models.

Appendix A

Kepler's Laws of Planetary Motion

In this appendix we prove Kepler's laws of planetary motion.

A.1 Kepler's 2nd Law

Theorem (Law of Equal Areas). *The area element, dA , swept out by the star-planet radius vector in the time interval, dt , is given*

$$\dot{A} = \frac{dA}{dt} = \text{constant}.$$

Proof. Suppose that there are two particles P_1, P_2 with mass m_1, m_2 , and with position vectors \vec{r}_1, \vec{r}_2 referred to some origin O fixed in inertial space. Moreover, let vector $\vec{r} = \vec{r}_2 - \vec{r}_1$ denotes the relative position of the particle P_2 with respect to P_1 and $|\vec{r}| = r$ (see Figure A.1).

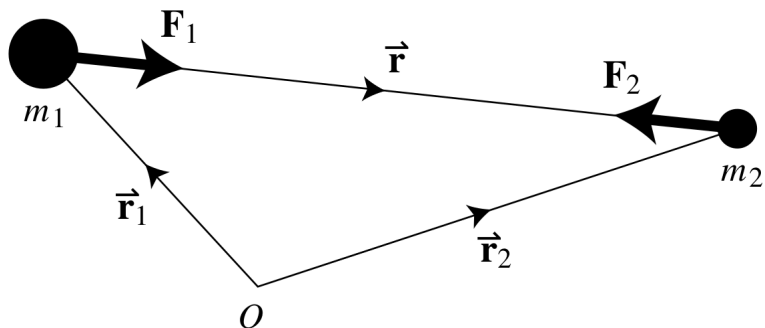


Figure A.1: A vector diagram for the forces acting on two particles ([10], p.23).

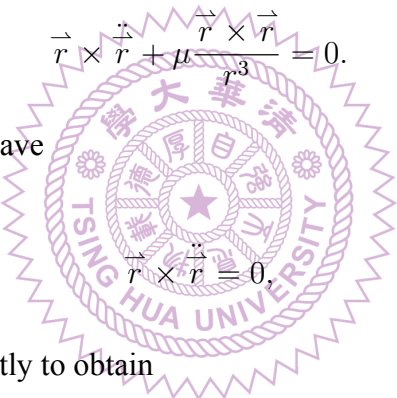
Then the gravitational forces and the consequent accelerations experienced by the two particles are

$$\mathbf{F}_1 = m_1 \ddot{\vec{r}}_1 = +G \frac{m_1 m_2 \vec{r}}{r^3} \quad \text{and} \quad \mathbf{F}_2 = m_2 \ddot{\vec{r}}_2 = -G \frac{m_1 m_2 \vec{r}}{r^3}, \quad (\text{A.1})$$

where G is the universal gravitational constant. From Eq.(A.1) we could obtain the equation of relative motion,

$$\frac{d^2 \vec{r}}{dt^2} + \mu \frac{\vec{r}}{r^3} = 0, \quad (\text{A.2})$$

where $\mu = G(m_1 + m_2)$. If we make an outer product of \vec{r} with Eq.(A.2), then we have the following equations



$$\vec{r} \times \ddot{\vec{r}} + \mu \frac{\vec{r} \times \vec{r}}{r^3} = 0. \quad (\text{A.3})$$

Since $\vec{r} \times \vec{r}$ is equal to 0, we have

$$\vec{r} \times \ddot{\vec{r}} = 0, \quad (\text{A.4})$$

which could be integrated directly to obtain

$$\vec{r} \times \dot{\vec{r}} = \vec{h}, \quad (\text{A.5})$$

where \vec{h} is a constant vector.

Now, we transform to a polar coordinate system $(\hat{r}, \hat{\theta})$ referred to an origin centred on the particle P_1 and an arbitrary reference line corresponding to $\theta = 0$. We used notation for Cartesian unit vectors uses the letters $\hat{i}, \hat{j}, \hat{k}$, and define the unit vectors \hat{r} and $\hat{\theta}$ along and perpendicular to the radius vector \vec{r} respectively, i.e.

$$\begin{cases} \hat{r} = \cos(\theta)\hat{i} + \sin(\theta)\hat{j} \\ \hat{\theta} = -\sin(\theta)\hat{i} + \cos(\theta)\hat{j}. \end{cases}$$

Then the vector \vec{r} can be written in polar coordinates as

$$\vec{r} = r\hat{r}. \quad (\text{A.6})$$

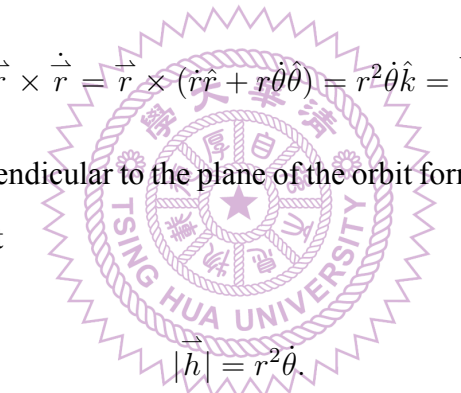
We differentiate Eq.(A.6) with respect to the time t , then we have

$$\dot{\vec{r}} = \dot{r}\hat{r} + r\dot{\theta}\hat{\theta}. \quad (\text{A.7})$$

The second derivative of \vec{r} can be obtained as

$$\ddot{\vec{r}} = (\ddot{r} - r\dot{\theta}^2)\hat{r} + (r\ddot{\theta} + 2\dot{r}\dot{\theta})\hat{\theta} = (\ddot{r} - r\dot{\theta}^2)\hat{r} + \left(\frac{1}{r}\frac{d}{dt}(r^2\dot{\theta})\right)\hat{\theta}. \quad (\text{A.8})$$

If we make the outer product into Eq.(A.7), from Eq.(A.5), then we have



$$\vec{r} \times \dot{\vec{r}} = \vec{r} \times (r\dot{\hat{r}} + r\dot{\theta}\hat{\theta}) = r^2\dot{\theta}\hat{k} = \vec{h}, \quad (\text{A.9})$$

$$|\vec{h}| = r^2\dot{\theta}. \quad (\text{A.10})$$

Consider the motion of the particle P_2 during a time interval dt . The areal velocity of the small triangle area A having base r and height $r\dot{\theta}$ swept out by the radius vector in time dt is

$$\frac{dA}{dt} = \frac{1}{2}r \cdot r\dot{\theta} = \frac{1}{2}r^2\dot{\theta} = \frac{1}{2}|\vec{h}|. \quad (\text{A.11})$$

From Eq.(A.5), we conclude that $\frac{dA}{dt}$ is constant. Therefore Eq.(A.11) prove that equal areas are swept out in equal times, that is, Kepler's 2nd Law ([10], p.25). \square

A.2 Kepler's 1st Law

Theorem (Law of Ellipses). *Let star-planet radius vector denote \vec{r} . Then, in polar coordinate system,*

$$|\vec{r}| = r = \frac{p}{1 + e \cos(\theta - \varpi)},$$

where e , ϖ , and p are arbitrary constants.

Proof. From Eq.(A.2) and Eq.(A.8), we have

$$\ddot{\vec{r}} = (\ddot{r} - r\dot{\theta}^2)\hat{r} + \left(\frac{1}{r}\frac{d}{dt}(r^2\dot{\theta})\right)\hat{\theta} = (\ddot{r} - r\dot{\theta}^2)\hat{r} + 0 = -\frac{\mu}{r^2}\hat{r}. \quad (\text{A.12})$$

From Eq.(A.12), we obtain

$$(\ddot{r} - r\dot{\theta}^2) = -\frac{\mu}{r^2}. \quad (\text{A.13})$$

To get the equation of the orbit, we let $u = 1/r$ and use the result from Eq.(A.10). Then the first derivative and second derivative of r are

$$\dot{r} = \frac{d}{dt}\left(\frac{1}{u}\right) = -\frac{1}{u^2}\frac{du}{dt} = -\frac{1}{u^2}\frac{du}{d\theta}\frac{d\theta}{dt} = -r^2\dot{\theta}\frac{du}{d\theta} = -|\vec{h}|\frac{du}{d\theta},$$

and

$$\ddot{r} = \frac{d}{dt}\left(-|\vec{h}|\frac{du}{d\theta}\right) = -|\vec{h}|\frac{d^2u}{d\theta^2}\frac{d\theta}{dt} = -|\vec{h}|\dot{\theta}\frac{d^2u}{d\theta^2} = -|\vec{h}|\cdot\frac{|\vec{h}|}{r^2}\frac{d^2u}{d\theta^2} = -|\vec{h}|^2u^2\frac{d^2u}{d\theta^2}.$$

We could rewrite Eq.(A.13) to obtain

$$(-|\vec{h}|^2u^2\frac{d^2u}{d\theta^2} - \frac{1}{u}\dot{\theta}^2) = -\mu u^2. \quad (\text{A.14})$$

Moreover, we multiply both sides of Eq.(A.14) by $-1/(u^3)$. Then we have

$$|\vec{h}|^2\frac{1}{u}\frac{d^2u}{d\theta^2} + \frac{1}{u^4}\dot{\theta}^2 = \frac{\mu}{u}.$$

From the result of Eq.(A.10), we get

$$|\vec{h}|^2\frac{1}{u}\frac{d^2u}{d\theta^2} + |\vec{h}|^2 = \frac{\mu}{u}. \quad (\text{A.15})$$

Additionally, we multiply both sides of Eq.(A.15) by $\vec{u}/(\vec{h}^2)$. Then we obtain

$$\frac{d^2u}{d\theta^2} + u = \frac{\mu}{|\vec{h}|^2}, \quad (\text{A.16})$$

which is the differential equation of the orbit of a particle moving ([2], p.231).

We solve the second-order differential equation of Eq.(A.16). Then the solution is

$$\begin{aligned} u &= \frac{\mu}{|\vec{h}|^2} + (A \cos(\theta) + B \sin(\theta)) \\ &= \frac{\mu}{|\vec{h}|^2} + (A' \cos(\varpi) \cos(\theta) + B' \sin(\varpi) \sin(\theta)) \\ &= \frac{\mu}{|\vec{h}|^2} + D \cos(\theta - \varpi), \end{aligned} \quad (\text{A.17})$$

where ϖ, A, B, A', B' , and D are constants.

Let $D = e\mu/(\vec{h}^2)$ for each $e \in \mathbb{R}$. Then from Eq.(A.17), we have

$$u = \frac{\mu}{|\vec{h}|^2} (1 + e \cos(\theta - \varpi)). \quad (\text{A.18})$$

Therefore, we substitute $u = 1/r$ into Eq.(A.18), then we obtain

$$r = \frac{p}{1 + e \cos(\theta - \varpi)}, \quad (\text{A.19})$$

where $p = |\vec{h}|^2/\mu$. We have proven Kepler's 1st Law already. \square

Eq.(A.19) is the general equation of a conic in polar coordinates where e is the eccentricity and p is the semilatus rectum. We let a be the semi-major axis of the conic and q be the closest distance to the central particle.

Type	The value of e	The value of p
Circle	$e = 0$	$p = a$
Ellipse	$0 < e < 1$	$p = a(1 - e^2)$
Parabola	$e = 1$	$p = 2q$
Hyperbola	$e > 1$	$p = a(e^2 - 1)$

Table A.1: Types of orbit ([10], p.26).

In Table A.1, the definition of different types of orbits. For example, if the eccentricity is equal

to 0 and the semilatus rectum p is equal to the semi-major axis a , then the orbit is circle. Other types of orbits are presented in Table A.1.

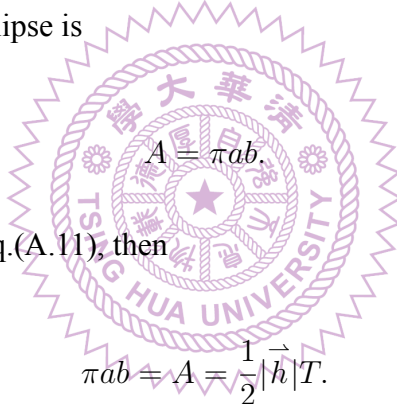
A.3 Kepler's 3rd Law

Theorem (The Harmonic Law). *Consider a elliptical orbital planet motion and its orbital period is T . If a is the semi-major axis of the elliptical orbit, then*

$$T^2 = ca^3,$$

where c is arbitrary constant.

Proof. Let b be the semi-minor axis of the elliptical orbit. Then from the formula for area of the ellipse, the area A of the ellipse is



Furthermore, if we integrate Eq.(A.11), then

$$\pi ab = A = \frac{1}{2} |\vec{h}| T. \quad (\text{A.20})$$

We square both sides of Eq.(A.20). Then we obtain

$$(\pi ab)^2 = \frac{1}{4} |\vec{h}|^2 T^2. \quad (\text{A.21})$$

Suppose that p is the semilatus rectum and e is the eccentricity. Let $p = |\vec{h}|^2 / \mu$ from Eq.(A.19) and use the result of Eq.(A.21). We could have

$$T^2 = \frac{4\pi^2 a^2 b^2}{|\vec{h}|^2} = \frac{4\pi^2 a^2 b^2}{p\mu}.$$

From Table A.1, p of the elliptical orbit is equal to $a(1 - e^2)$. Then we obtain

$$T^2 = \frac{4\pi^2 a^2 b^2}{p\mu} = \frac{4\pi^2 a^2 b^2}{\mu a(1 - e^2)}.$$

Since $b = (1 - e^2)^{1/2}a$, then

$$T^2 = \frac{4\pi^2 a^2 b^2}{\mu a(1 - e^2)} = \frac{4\pi^2 a^2 (a^2(1 - e^2))}{\mu a(1 - e^2)} = \frac{4\pi^2}{\mu} a^3. \quad (\text{A.22})$$

Therefore, Eq.(A.22) is the mathematical form of Kepler's 3rd Law. \square



Appendix B

Three Dimensional Transformation

In this appendix we show the transformation of the orbital plane system $(\hat{x}, \hat{y}, \hat{z})$ to the general reference system $(\hat{X}, \hat{Y}, \hat{Z})$.

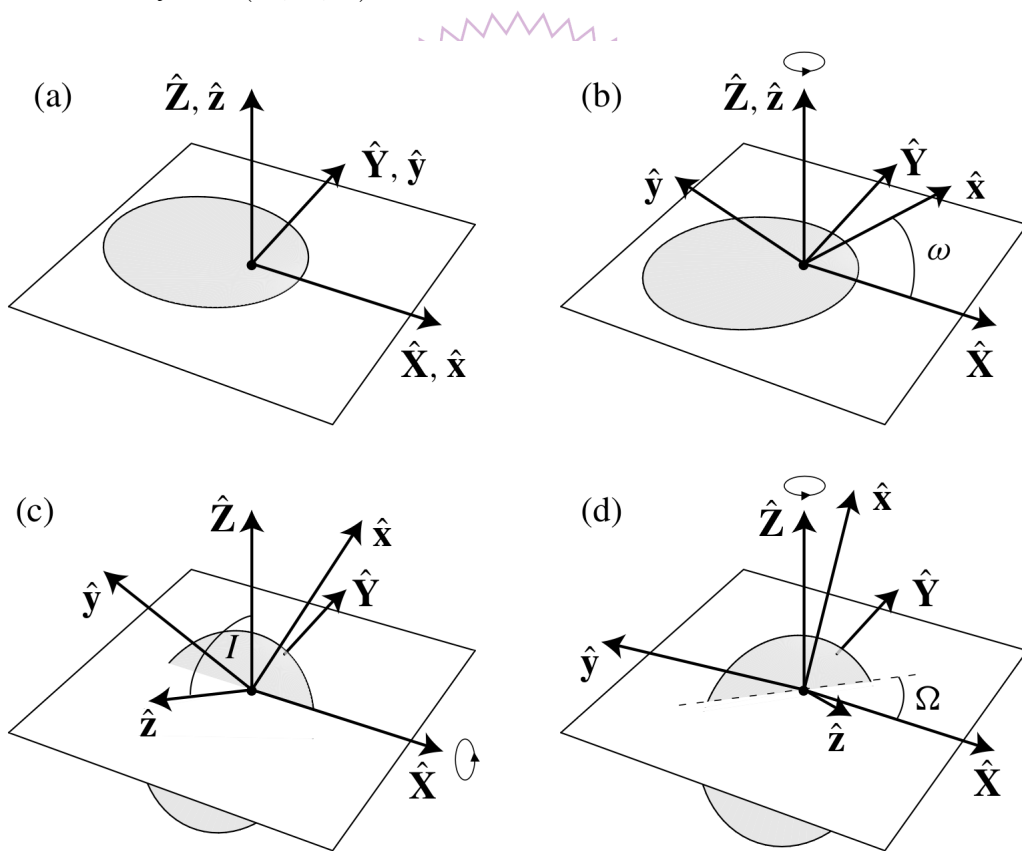


Figure B.1: The relation between the orbital plane system $(\hat{x}, \hat{y}, \hat{z})$ and the reference plane system $(\hat{X}, \hat{Y}, \hat{Z})$ ([10], p.50). (a) The originally coincident axes. (b) The first rotation. (c) The second rotation. (d) The final rotation.

The first rotation is through a positive angle ω about the \hat{Z} axis (see Figure B.1.b). We could

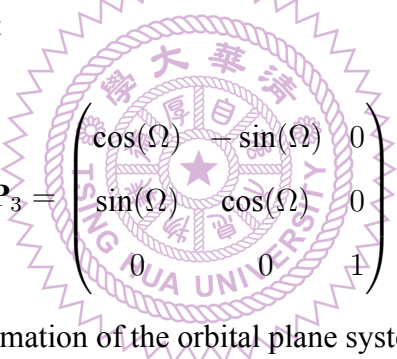
represent the transformation by a rotation matrix, which defined

$$\mathbf{P}_1 = \begin{pmatrix} \cos(\omega) & -\sin(\omega) & 0 \\ \sin(\omega) & \cos(\omega) & 0 \\ 0 & 0 & 1 \end{pmatrix}.$$

The second rotation is through a positive angle I about the \hat{X} axis (see Figure B.1.c). Then we define the second rotation matrix i.e.

$$\mathbf{P}_2 = \begin{pmatrix} 1 & 0 & 0 \\ 0 & \cos(I) & -\sin(I) \\ 0 & \sin(I) & \cos(I) \end{pmatrix}.$$

Finally, the final rotation is through a positive angle Ω about the \hat{Z} axis (see Figure B.1.d). We suppose the rotation matrix that



$$\mathbf{P}_3 = \begin{pmatrix} \cos(\Omega) & -\sin(\Omega) & 0 \\ \sin(\Omega) & \cos(\Omega) & 0 \\ 0 & 0 & 1 \end{pmatrix}.$$

Therefore, the series of transformation of the orbital plane system to the general reference system is

$$\begin{pmatrix} \hat{X} \\ \hat{Y} \\ \hat{Z} \end{pmatrix} = \mathbf{P}_3 \mathbf{P}_2 \mathbf{P}_1 \begin{pmatrix} \hat{x} \\ \hat{y} \\ \hat{z} \end{pmatrix}.$$

Furthermore, since the rotation matrices are invertible, we could write inverse transformation as

$$\begin{pmatrix} \hat{x} \\ \hat{y} \\ \hat{z} \end{pmatrix} = \mathbf{P}_1^{-1} \mathbf{P}_2^{-1} \mathbf{P}_3^{-1} \begin{pmatrix} \hat{X} \\ \hat{Y} \\ \hat{Z} \end{pmatrix}.$$

References

- [1] James Binney and Scott Tremaine. *Galactic dynamics*, volume 13. Princeton university press, 2011.
- [2] G.R. Fowles and G.L. Cassiday. *Analytical Mechanics*. Analytical Mechanics. Thomson Brooks/Cole, 2005.
- [3] Ing-Guey Jiang and Li-Chin Yeh. Galaxies with supermassive binary black holes:(i) a possible model for the centers of core galaxies. *Astrophysics and Space Science*, 349(2):881–893, 2014.
- [4] Henry E Kandrup, Ioannis V Sideris, Balša Terzić, and Courtlandt L Bohn. Supermassive black hole binaries as galactic blenders. *The Astrophysical Journal*, 597(1):111, 2003.
- [5] Marc L Kutner. *Astronomy: A physical perspective*. Cambridge University Press, 2003.
- [6] Tod R Lauer, Edward A Ajhar, Y-I Byun, Alan Dressler, SM Faber, Carl Grillmair, John Kormendy, Douglas Richstone, and Scott Tremaine. The centers of early-type galaxies with hst. i. an observational survey. *Astronomical Journal v. 110, p. 2622*, 110:2622, 1995.
- [7] Miloš Milosavljević and David Merritt. Formation of galactic nuclei. *The Astrophysical Journal*, 563(1):34, 2001.
- [8] Jeremy D Murphy, Karl Gebhardt, and Joshua J Adams. Galaxy kinematics with virus-p: the dark matter halo of m87. *The Astrophysical Journal*, 729(2):129, 2011.
- [9] Carl D Murray and Alexandre CM Correia. Keplerian orbits and dynamics of exoplanets. *Exoplanets*, pages 15–23, 2010.
- [10] Carl D Murray and Stanley F Dermott. *Solar system dynamics*. Cambridge university press, 1999.
- [11] Jian-Min Wang, Yan-Mei Chen, Chen Hu, Wei-Ming Mao, Shu Zhang, and Wei-Hao Bian. Active galactic nuclei with double-peaked narrow lines: are they dual active galactic nuclei? *The Astrophysical Journal*, 705(1):L76, 2009.
- [12] Li-Chin Yeh and Guey Jiang. Studying dynamical models of the core galaxy ngc 1399 with merging remnants. *Research in Astronomy and Astrophysics*, 18(12):153, 2018.